METEORITICS & PLANETARY SCIENCE

Heating experiments of the Tagish Lake meteorite: investigation of the effects of short-term heating on chondritic organics

Journal:	*Meteoritics & Planetary Science*
Manuscript ID	MAPS-2971.R1
Manuscript Type:	Article
Date Submitted by the Author:	n/a
Complete List of Authors:	Chan, Queenie Hoi Shan Nakato, Aiko; Kyoto University Kebukawa, Yoko; Carnegie Institution of Washington, Geophysical Laboratory Zolensky, Michael; NASA Johnson Space Center, Nakamura, Tomoki; Tohoku University, Department of Earth and Planetary Materials Science, Faculty of Science Maisano, Jessie; U T Austin, Colbert, Matthew ; U T Austin Martinez, James; Jacobs, Kilcoyne, David; LBNL, SSG Suga, Hiroki; Hiroshima University, Department of Earth and Planetary Systems Science Takahashi, Yoshio ; The University of Tokyo, Department of Earth and Planetary Science Takeichi, Yasuo; High-Energy Accelerator Research Organization ; Graduate University for Advanced Studies Mase, Kazuhiko; High-Energy Accelerator Research Organization ; Graduate University for Advanced Studies Wright, Ian; Open University, Physical Sciences
Keywords:	Organic matter, Spectroscopy, alteration < Thermal, Space mission(s)

Note: The following files were submitted by the author for peer review, but cannot be converted to PDF. You must view these files (e.g. movies) online.

Movie S1.avi
Movie S2.avi

Heating experiments of the Tagish Lake meteorite: investigation of the effects of short-term heating on chondritic organics

Queenie H. S. Chan[1]*†, Aiko Nakato[2], Yoko Kebukawa[3], Michael E. Zolensky[1], Tomoki Nakamura[4], Jessica A. Maisano[5], Matthew W. Colbert[5], James E. Martinez[6], A.L. David Kilcoyne[7], Hiroki Suga[8], Yoshio Takahashi[9], Yasuo Takeichi[10,11], Kazuhiko Mase[10,11] and Ian P. Wright[1]

[1]ARES, NASA Johnson Space Center, Houston, Texas 77058, USA

[2]Graduate School of Science, Kyoto University, Kitashirakawa Oiwake-cho, Sakyo-ku, Kyoto 606-8502, Japan

[3]Faculty of Engineering, Yokohama National University, 79-5 Tokiwadai, Hodogayaku, Yokohama 240-8501, Japan

[4]Graduate School of Science, Tohoku University, Sendai, Miyagi 980-8578, Japan

[5]Department of Geological Sciences, Jackson School of Geosciences, The University of Texas, Austin, TX 78712, USA

[6]Jacobs Engineering, Houston, TX 77058, USA

[7]Advanced Light Source, Lawrence Berkeley National Laboratory, 1 Cyclotron Road, Berkeley, CA 94720, USA

[8]Department of Earth and Planetary Systems Science, Hiroshima University, Kagamiyama, Higashi-Hiroshima, Hiroshima 739-8526, Japan

[9]Department of Earth and Planetary Science, The University of Tokyo, Hongo, Bunkyo-ku, Tokyo 113-0033, Japan

[10]Institute of Materials Structure Science, High-Energy Accelerator Research Organization (KEK), 1-1 Oho, Tsukuba, Ibaraki 305-0801, Japan

[11]Department of Materials Structure Science, SOKENDAI (The Graduate University for Advanced Studies)

*Corresponding author: Queenie H. S. Chan (E-mail: queenie.chan@open.ac.uk; Telephone: +1 (585) 653-6144).

†Current address: Department of Physical Sciences, The Open University, Walton Hall, Milton Keynes, MK7 6AA, UK

ABSTRACT

We present in this study the effects of short-term heating on organics in the Tagish Lake meteorite and how the difference in the heating conditions can modify the organic matter (OM) in a way that complicates the interpretation of a parent body's heating extent with common cosmothermometers. The kinetics of short-term heating and its influence on the organic structure are not well understood, and any study of OM is further complicated by the complex alteration processes of the thermally metamorphosed carbonaceous chondrites – potential analogues of the target asteroid Ryugu of the Hayabusa2 mission – which had experienced post-hydration, short-duration local heating. In an attempt to understand the effects of short-term heating on chondritic OM, we investigated the change in the OM contents of the experimentally heated Tagish Lake meteorite samples using Raman spectroscopy, scanning transmission X-ray microscopy utilizing X-ray absorption near edge structure spectroscopy, and ultra-performance liquid chromatography fluorescence detection and quadrupole time of flight hybrid mass spectrometry. Our experiment suggests that graphitization of OM did not take place despite the samples being heated to 900°C for 96 hours, as the OM maturity trend was influenced by the nature of the OM precursor, such as the presence of abundant oxygenated moieties. Although both the intensity of the 1s−σ* exciton cannot be used to accurately interpret the peak metamorphic temperature of the experimentally heated Tagish Lake sample, the Raman graphite band widths of the heated products significantly differ from that of chondritic OM modified by long-term internal heating.

1 INTRODUCTION

Carbonaceous chondrites exhibit a wide range of aqueous and thermal alteration characteristics, while some are known to demonstrate mineralogical and petrologic evidence of having been thermally metamorphosed after aqueous alteration. Their occurrences challenge the initial view of which carbonaceous chondrites, that have experienced pervasive aqueous alteration, were not extensively heated. This group of dehydrated meteorites are commonly referred as thermally metamorphosed carbonaceous chondrites (TMCCs), and their relatively flat visible near infrared reflectance spectra resemble that of C-, G-, B- and F-type asteroids that typically have low albedos (Gaffey et al. 1989; Hiroi et al. 1993; Hiroi et al. 1996). The surfaces of these dark asteroids, which include the C- and B-type target asteroids – Ryugu and Bennu of the ongoing sample return missions, Hayabusa2 and OSIRIS-REx, respectively – are potentially composed of both hydrous and dehydrated minerals, and thus TMCCs are among the best samples that can be studied in the laboratory to reveal the true nature of these carbonaceous asteroids.

Although many TMCCs were previously categorized as Ivuna-type (CI) and Mighei-type (CM) chondrites, they are not strictly CI/CM because they exhibit isotopic and petrographic characteristics that significantly deviate from typical CI/CM, and hence were given the term “CI-/CM-like chondrites”. TMCCs consist mainly of dehydrated phyllosilicates, have higher bulk O isotopic compositions (CI-/CM-like chondrites: $\delta^{17}O$ = +9 to 12‰, $\delta^{18}O$ = +17 to 22‰; CM chondrites: $\delta^{17}O$ = –1 to +3‰, $\delta^{18}O$ = +5 to 11‰), and lower H_2O and C contents relative to CI/CM chondrites (Clayton and Mayeda 1999; Ikeda 1992; Tonui et al. 2014). Examples of TMCCs include the C2-ung/CM2TIV Belgica (B)-7904, Yamato (Y-), Y-82162, Y-86720, Y-980115 and Wisconsin Range (WIS) 91600 (e.g., Akai 1988; Burton et al. 2014; Chan et al. 2016a; Ikeda 1991, 1992; King et al. 2015b; Nakamura 2005; Nakato et al. 2008; Tomeoka et al. 1989a, b; Tonui et al. 2014). Thermal alteration is virtually complete in B-7904 and Y-86720, thus they are considered typical end-members of TMCCs exhibiting complete dehydration of matrix phyllosilicates (Nakamura 2005; Tonui et al. 2014). The estimated heating durations of TMCCs are surprisingly short when compared to parent body heating with heat sources derived from *in situ* decay of radionuclides that could last millions of years. The heating conditions of TMCCs

were estimated to be 10 to 10^3 days at 700°C to 1 to 100 hours at 890°C, which suggest that they have experienced short-term heating possibly induced by impact and/or solar radiation (Chan et al. 2017b; Nakato et al. 2008; Yabuta et al. 2010).

While the petrology and chemistry of TMCCs have only recently been extensively characterized, we have just begun to study in detail how short-term heating influences their organic contents. We investigated the change in the organic content of the carbonate-poor lithology of experimentally heated Tagish Lake C2 meteorite, as the chemical and bulk oxygen (O) isotopic compositions ($\delta^{17}O$ = +8 to 9‰, $\delta^{18}O$ = +18 to 19‰) of this lithology bear similarities to that of the TMCCs (Clayton and Mayeda 2001; Engrand et al. 2001; Zolensky et al. 2002). The Tagish Lake meteorite has a bulk carbon (C) content of approximately 4 wt%, of which about <2 wt% comes from IOM and <1 wt% from carbonate C (Alexander et al. 2014; Pearson et al. 2006). Carbonates are relatively uncommon in the carbonate-poor lithology which occur as sparse fine polycrystalline grains of <5 μm (Zolensky et al. 2002), so the contribution of carbonate C to the bulk C content is expected to be lower in this lithology. The carbonate-poor lithology also contains abundant organic nanoglobules with aliphatic and oxygenated function groups that have elevated δD and $\delta^{15}N$ values, which suggests a highly primitive, possibly presolar origin for the organics, and their formation in the cold molecular clouds and the outer protosolar disk at extremely low temperatures (<–250°C) (Nakamura-Messenger et al. 2006; Nakamura et al. 2002). The bulk O isotopic composition and the presence of organic nanoglobules indicate that aqueous alteration occurred at low temperatures (<100°C) (Zolensky et al. 2002). The isotopic compositions (δD = +815 to 1844‰, $\delta^{13}C$ = –14.7 to –13.3 ‰, $\delta^{15}N$ = +53 to 57) of the IOM extracted from the Tagish Lake meteorite are intermediate between that of the IOM in typical CI, CM and Renazzo-type (CR) chondrites (Alexander et al. 2014; Herd et al. 2011). The more aqueously-altered lithology are drawn closer to the least metamorphosed ordinary chondrites (OC), Vigarano-type (CV), and Ornans-type (CO) chondrites, which suggests that the isotopic variation was to a certain extent influenced by aqueous alteration. Nevertheless, only limited changes were observed for the C content, isotopic, and structural properties of the IOM in the Tagish Lake meteorite samples that exhibit different extents of aqueous alteration, which offers another line of evidence towards a low temperature alteration history (Alexander et al. 2014; Yabuta et al. 2007).

The low temperature aqueous alteration history of the Tagish Lake meteorite, its moderate IOM abundance relatively unaltered by aqueous processing, and its quick retrieval (frozen) upon an observed fall event without direct hand contact (Brown et al. 2000), justify this meteorite as the perfect and organically pristine candidate for the study of the change in the OM content by experimental heating. With the use of Raman spectroscopy, scanning transmission X-ray microscopy (STXM) utilizing X-ray absorption near edge structure (XANES) spectroscopy, and ultra-performance liquid chromatography fluorescence detection and quadrupole time of flight hybrid mass spectrometry (UPLC-FD/QToF-MS), we analyzed the compositions of the organic solids and the amino acid contents of the experimentally heated (short-term heating) Tagish Lake samples in detail.

2 SAMPLES AND METHODS

The Tagish Lake meteorite has two main lithologies – carbonate-poor (the dominant lithology) and carbonate-rich (less abundant lithology) (Zolensky et al. 2002) (Figure 1). Different Tagish Lake meteorite fragments also exhibit a wide variation in the organic content that correlates to the extent of parent body aqueous alteration (Tagish Lake specimens showing an increasing degree of aqueous alteration: 5b [the least aqueously altered] < 11h < 11i < 11v [the most aqueously altered]), where the amino acid abundances are higher in the fragments which show a lower degree of aqueous alteration, while the IOM C contents only decrease slightly with a considerable increase in the aromatic content in the more aqueously-altered lithology (e.g., Alexander et al. 2014; Glavin et al. 2012; Herd et al. 2011).

To ensure that our heating experiments and the interpretation of the resulting organic content were not significantly influenced by sample heterogeneity, we selected only the carbonate-poor lithology of the Tagish Lake meteorite (#11). The carbonate-poor lithology was located by mineral identification via X-ray computed tomography (XRCT) at the High-Resolution X-ray Computed Tomography Facility at The University of Texas at Austin. Tomographic imaging was critical in identifying internal lithologic and mineralogical differences, which we used to decide where to make the initial slice into the sample and prepare thin sections. The initial samples were then characterized by scanning electron microscopy (SEM) and energy-dispersive spectrometry (EDS) to verify the carbonate-poor lithology based on elemental mapping and comparison to the XRCT images (Figure 1).

We then subsampled the carbonate-poor lithology into four equal portions, each weighing approximately 200 mg. Half of the samples was used in this study, while the other half was analyzed to determine the variation in chemical, petrography, mineralogy, and bulk O isotope compositions upon heating, using synchrotron X-ray diffraction (XRD) analysis at the High Energy Accelerator Research Organization (KEK) using beam line BL-3A, and SEM/EDS, electron probe micro-analyzer equipped with a wavelength dispersive spectrometer (EPMA/WDS), transmission electron microscopy (TEM) and laser fluorination mass spectrometer at JAXA/ISAS. The results of the second portion of the sample are discussed in Nakato et al. (2016).

2.1 XRCT

The Tagish Lake meteorite sample was scanned at the University of Texas High-Resolution X-ray Computed Tomography Facility using the Xradia microXCT Scanner (Zeiss). The detector permits cone-beam acquisition, and under the ultra high-resolution mode, 882 slices were collected covering the entire scan volume in a single rotation. Images were obtained by relatively low-energy X-rays (80kV), 10W, 2.5 s acquisition time, with a spatial resolution (voxel size) of 46 μm.

2.2 SEM/EDS

Secondary electron (SE) imaging and mineral elemental compositions were obtained using the Zeiss SUPRA 55VP field-emission (FE) SEM at the Structural Engineering Division, NASA Johnson Space Center (JSC) (Figure S1). Fragments of the Tagish Lake meteorite were mounted in indium and prepared in the same manner as described in Chan et al. (2016b). The SEM parameters were: Accelerating voltage = 20 kV; Aperture = 120 mm (largest); High current mode = on; Beam size = approximately 3 to 5 nm; Incident beam current = 9.2 to 9.3 nA; Working distance ≈ 6 mm.

2.3 Heating experiments

Subsamples (~100 mg) of the carbonate-poor Tagish Lake lithology were subjected to heating experiments at 600° and 900°C for 1 and 96 hours: (1) 600°C/1h, (2) 600°C/96h, (3) 900°C/1h, and (4) 900°C/96h. During the experiments, the heating chamber was kept under a controlled environment. To reproduce the secondary iron-bearing minerals in B-7904 heated chondrite that contains both Fe and Fe^{2+}, a Fe metal rod was put in the chamber with the O fugacity kept at the condition closer to that of the iron-wüstite (IW) buffer. The estimated pressure was below 5×10^{-5} Pa. The detailed experimental configuration is shown in Nakato et al. (2008).

2.4 Raman spectroscopy

The unheated and heated Tagish Lake samples were analyzed using a Jobin-Yvon Horiba LabRam HR (800 mm) Raman microprobe at NASA JSC. The excitation source was a 514 nm (green) laser. The slit width and the confocal pinhole aperture were set at 100 μm and 200 μm, respectively, and an 1800 grooves/mm grating was used to disperse the Raman signal. The laser beam was focused through a microscope equipped with an 80× objective (numerical aperture = 0.75), and the

Raman backscattered light was collected from the same objective. At this magnification and for the laser used, the minimum achievable spot size was approximately 1 μm, and the laser power at the sample surface was ≤450 μW. At least 12 spectra were collected on each raw matrix grain (flattened between two glass slides) in the spectral range of 100–4000 cm^{-1}. This spectral range includes the first- and second-order Raman bands of carbon. The exposure time for each spectrum was 15s and three accumulations were obtained for each analytical spot to identify and discard spurious signals, such as those from cosmic rays, leading to a total acquisition time of up to 450 s with the use of an Extended Range option to collect data in various spectral windows.

The peak position (ω) and full width half-maximum (FWHM, Γ) of each Raman band were determined by simultaneous peak fitting to the two-peak Lorentzian and Breit–Wigner-Fano (BWF) model (Ferrari and Robertson 2000) with a linear baseline correction (Figure S2 and Figure S3). Wavelength calibration against a silicon wafer sample was checked daily prior to sample analyses. Details of the Raman technique are given in Chan et al. (2017b) and Kebukawa et al. (2017).

2.5 STXM-XANES

Focused ion beam (FIB) thin sections of the heated and unheated Tagish Lake samples were prepared using a FIB (Hitachi, FB2200) at ISAS/JAXA for three STXM-XANES analyses (2016 Feb, 2016 May and 2016 Dec). We subsampled FIB sections for each STXM-XANES analysis in order to investigate the sample heterogeneity. C-XANES measurements were performed using the compact-STXM installed at BL-13A beamline of the Photon Factory (PF), High Energy Accelerator Research Organization (KEK), and the STXM installed at beamline 5.3.2.2 of the Advanced Light Source, Lawrence Berkeley National Laboratory. The details of these instruments are described in Kilcoyne et al. (2003) and Takeichi et al. (2016). The C-XANES spectra were acquired using a ‘‘Stacks” method, with the energy step sizes of 0.1 eV in the region of 283–295.5 eV, 0.5 eV in the regions of 280–283 eV and 295.5–301.0 eV, and 1 eV in the region of 301–310 eV. The acquisition time for each energy step varied from 1 to 5 ms. The C-XANES spectra were corrected with background and analyzed by the subtraction of a linear regression using aXis2000 software, and then normalized to the intensity at 292 eV.

2.6 UPLC-FD/QToF-MS

The amino acid extraction was conducted at NASA JSC in the same manner as described in Chan et al. (2018). Porcelain mortars and pestles were scrubbed and washed with dilute soap solution, rinsed with Millipore Integral 10 UV (18.2 MΩ cm, <3 parts-per-billion [ppb] total organic carbon) ultrapure water, hereafter referred to as "water", immersed in 20% citric acid and sonicated at room temperature for 60 min. All tools, glassware, and ceramics were rinsed with water, wrapped in aluminum foil, and sterilized by heating in air at 500 °C for 24 h. Volumetric flasks were only rinsed with copious water. Amino acid standards and other laboratory chemicals such as ammonium hydroxide (NH_4OH) (28–30 wt %), sodium hydroxide (NaOH), hydrochloric acid (HCl) (37 %), methanol, hydrazine monohydrochloride, *o*-phthaldialdehyde (OPA), *N*-acetyl-L-cysteine (NAC) were obtained from Fischer Scientific, Sigma-Aldrich, or Acros Organics. Poly-Prep® prepacked ion exchange columns (AG 50W-X8 resin, 200–400 mesh, hydrogen form) were obtained from Bio-Rad. Solutions of sodium borate were prepared from solid sodium tetraborate decahydrate (Sigma Ultra 99.5–100% purity) that was heated in air at 500 °C for 24 h prior to dissolution in water. Amino acid standard solutions were made by dissolving individual amino acid solutes in water, and were combined into a standard mixture analyzed by UPLC-FD/QToF-MS on a daily basis.

The unheated and heated Tagish Lake meteorite samples were powdered and transferred to individual glass ampoules. Sterilized (500°C, 24h) laboratory quartz samples were subjected to the same heating experiment and amino acid extraction procedures and analyzed as procedural blanks.

One mL of water was added to each glass ampoule containing separate samples, and the ampoules were flame-sealed and heated to 100 °C for 24 h in an oven. After the hot water extraction, the samples were cooled to room temperature and centrifuged for 5 min to separate water supernatant from solid particulate. Exactly half of the water supernatant (500 µL) was transferred to a small test tube (10 × 75 mm), dried under vacuum (Savant™ SPD131DDA SpeedVac™ Concentrator), flame-sealed in a larger test tube (20 × 150 mm) containing 6 N HCl, and then subjected to acid vapor hydrolysis for 3 h at 150 °C in order to liberate amino acids in bound or precursor forms. After the vapor-hydrolysis procedure, the test tubes were

rinsed with water, and the bottom of the test tubes were opened to retrieve the inner small test tubes, and this portion of the sample is hereafter referred to as the "hydrolyzed extract", representing the total amino acid contents of the samples. The remaining hot-water extract was rinsed with 2 × 1 mL water and the supernatant was transferred to individual test tubes, this portion of the sample is hereafter referred to as the "non-hydrolyzed extract" (not described further in this study), containing only the free amino acids. Both hydrolyzed and non-hydrolyzed samples were then brought up in 3 × 1 mL of water and desalted on a cation exchange resin. Amino acids were eluted with 2 × 3.5 mL of 2 M NH_4OH. The eluates were collected in small test tubes and evaporated to dryness. The samples were transferred to small sample vials, re-dissolved in 100 µL of water, and stored at −20°C. Immediately before UPLC-FD/QToF-MS analysis, the samples were derivatized with OPA/NAC fluorescent derivatization (Glavin et al. 2006). 25 µL of the thawed sample was dried under vacuum, re-suspended in 20 µL 0.1 M sodium borate buffer (pH 9), and derivatized with 5 µL OPA/NAC in 1 mL autosampler glass vials. The derivatization reaction was then quenched after 15 min. at room temperature with 75 µL of 0.1 M hydrazine hydrate.

The amino acid abundances and distributions were measured by UPLC-FD/QToF-MS at NASA JSC, using a Waters ACQUITY ultrahigh performance LC and a Waters ACQUITY fluorescence detector connected in series to a Waters LCT Premier ToF-MS. 25 µL of the derivatized samples were separated using a Waters BEH C18 column (2.1 × 50 mm, 1.7 µm particle size) followed by a second Waters BEH phenyl column (2.1 × 150 mm, 1.7 µm particle size). Chromatographic conditions were: column temperature, 30°C; flow rate, 150 µL min^{-1}; solvent A (50 mM ammonium formate, 8% methanol, pH 8.0); solvent B (methanol); gradient, time in minutes (%B): 0 (0), 35 (55), 45 (100). The electrospray and mass spectrometer conditions have been described by Glavin et al. (2006). Amino acids in the samples were identified by correlating sample compounds with known standards using the representative masses and fluorescence responses of the OPA/NAC amino acid derivatives at the expected chromatographic retention times.

3 RESULTS

The Tagish Lake meteorite fragments heated under the four experiments show distinctive textural, mineralogical, structural, and chemical changes (Figure 2). The mineralogy and texture of the Tagish Lake samples heated at 900°C show the closest resemblance to that of the strongly heated TMCCs due to the dehydration of hydrous minerals such as phyllosilicates and formation of magnetite, and recrystallization back into anhydrous fine-grained (<100 nm) secondary olivine, pyroxene, Fe-Ni metal and troilite (Nakato et al. 2016). Therefore, while phyllosilicates (e.g. saponite and serpentine), magnetite and Fe-Ni sulfides are common mineral phases observed in the matrix of the unheated carbonate-poor lithology of the Tagish Lake meteorite (Zolensky et al. 2002), the Tagish Lake samples heated to 900°C show mineral assemblages of predominantly anhydrous silicates, metal and troilite, implying a reducing heating environment. Upon heating at 900°C, oxidation of organics by silicate O has reduced the total C contents of the Tagish Lake samples down to approximately 20% of that of the unheated counterpart, and thus the majority of the IOM was decomposed after heating (T. Nakamura, personal communication, 2018). This also accounts for the increase in the abundance of metallic Fe produced by the reduction of silicate FeO. The changes in mineralogical and isotopic compositions are discussed in more detail in a separate paper. In this paper, we focus on the changes observed in the organic contents of the meteorite fragments.

3.1 Raman C parameters of the Tagish Lake OM

3.1.1 *OM in the unheated Tagish Lake meteorite*

Carbonaceous materials feature Raman bands in the first- and second-order regions. The most typical peaks are the first-order defect (D) band at ~1350−1380 cm^{-1} and the graphite (G) band at ~1580−1590 cm^{-1} (Tuinstra and Koenig 1970a, b). The peak parameters of the D and G bands, such as the peak center locations (usually referred to as peak position, ω), peak widths in terms of full width half-maximum (FWHM, Γ), and the peak intensity ratios between the D and G bands (I_D/I_G), were documented to systematically correlate with various properties of OM in meteorites. The combination of these peak parameters describes the overall size distribution of the crystalline domains and the metamorphic history of the carbonaceous host (Aoya et al. 2010; Beyssac et al. 2002; Bonal et al. 2006; Bonal et al. 2007; Busemann et al.

2007; Chan et al. 2017b; Homma et al. 2015; Kouketsu et al. 2014; Quirico et al. 2003).

Due to the sample heterogeneity of the Tagish Lake meteorite (Zolensky et al. 2002), and the adoption of different analytical methods and peak fitting algorithm, the Raman parameters of the OM in the Tagish Lake meteorite reported by different studies (Busemann et al. 2007; Matrajt et al. 2004; Nakamura et al. 2002; Quirico et al. 2014) are not necessarily the same (Table S1). Nevertheless, all studies are in agreement that the IOM in the Tagish Lake meteorite contains abundant, highly-disordered organic material. We have also analyzed separately three of the unheated subsamples from the carbonate-poor lithology of the Tagish Lake meteorite, and the Raman peak parameters of the OM are consistent with this study (Figure 3).

3.1.2 Heating experiments

A reduction in the fluorescence background intensity was observed after the Tagish Lake meteorite samples were subjected to the short-term heating experiments (Figure 4a). The unheated Tagish Lake meteorite fragment has the highest Raman intensity across the 100−4000 cm^{-1} spectral range, which is accompanied by an intense fluorescence signal leading to a steep background slope in the first-order D and G bands spectral region between 1300−1600 cm^{-1}. Accordingly, the I_D/I_G ratio increases as the Tagish Lake meteorite sample was exposed to higher heating temperatures (Figure 3b; Figure 4b). However, while the Raman band parameters show a clear correlation to the heating temperature, heating duration affects these parameters to a lesser extent. For instance, while samples heated to 900°C for 96h (shown as the diagonal-line-patterned symbols in Figure 3) has a lower fluorescence intensity, lower Γ_D and ω_D values than the 1h counterparts, this trend is opposite for the samples heated to 600°C. The difference in the 1h and 96h heating durations might not be significant enough to cause any observable variation in the Raman signatures.

3.2 C-XANES analysis of the Tagish Lake OM

3.2.1 OM in the unheated Tagish Lake meteorite

C-XANES spectroscopy is useful for detecting organic functional groups albeit incapable of characterizing the structure of the entire organic molecule. The

OM in the Tagish Lake meteorite bears similarities to the IOM in the highly primitive CI, CR and CM carbonaceous chondrites (Alexander et al. 2014; Cody et al. 2008a; Le Guillou et al. 2014), in terms of the types and relative abundance of the chemical moieties. The C-XANES spectra of the unheated Tagish Lake meteorite sample (Figure 5a) reveal an absorption feature at ~285.0 eV that is assigned to the 1s–π* transition of alkenyl and aromatic (C=C) carbon (Cody et al. 2008a). The weak peak at around 286.5 eV indicates a minor contribution of ketones (C=O), and at ~287.5 eV indicates aliphatic carbon (CH_n). However, the 287.5 eV feature is not distinctive in the Tagish Lake meteorite, probably due to (1) the small H/C and aliphatic/aromatic ratios of the OM in the more aqueously-altered lithology of the Tagish Lake meteorite compared to those of primitive CC (e.g., Alexander et al. 2014; Herd et al. 2011), and/or (2) C-XANES is less sensitive to the aliphatic carbon in complex macromolecular OM. The highly aromatic rich nature of the OM suggests that this Tagish Lake sample is more comparable to the aqueously altered specimens such as 11v and 11i rather than 5b analyzed in previous studies (e.g., Herd et al. 2011). The peak centered at ~288.5 eV corresponds to a 1s–π* transition associated with carbonyl carbon in carboxyl moieties and esters (O–C=O) (Lessard et al. 2007). In some locations, a small peak at 290.5 eV can be observed, which is assigned to the 1s–π* of carbonate. Differences in the presence and intensities of the above-mentioned peaks measured on different days on FIB sections extracted from adjacent areas of the same sample chip indicate significant sample heterogeneity (Figure 5a).

3.2.2 Heating experiments

Due to the significant sample heterogeneity, it was difficult to directly correlate any systematic variation in the organic structure to the extent of heating (Figure 5). The aromatic feature (C=C) at ~285.0 eV was expected to be more prominent in the heated samples as thermal annealing typically converts sp^3 C into aromatic sp^2 C and leads to an increase in the size of the aromatic moieties (Derenne and Robert 2010; Dischler et al. 1983). However, as shown in Figure 5b, the 285.0 eV peak intensity of the 900°C samples (magenta and red lines) is not always higher than the unheated (black lines) or the 600°C samples (blue and green lines). We have also conducted C-XANES spectral fitting following the procedure described in (Bernard et al. 2010) (Figure 6), derived from Gaussian fits to the major X-ray absorption features, in order to provide better quantification estimates for the absorption band intensities.

An example of a decomposed spectrum is provided in Figure S4. However, we did not observe any distinct trend among the peak area ratios (carboxyl to aliphatic, ketone to aliphatic, and aromatic to aliphatic) across samples that were heated to different extents, as any apparent trend observed were compensated by the error bars which represent sample heterogeneity (Figure 6). In addition, no systematic change was observed for the aliphatic (CH_n at ~287.5 eV) and graphene (at ~291.6 eV) structures upon heating. A 1s–σ* exciton peak is expected if highly conjugated sp^2 bonded C domains were present, as in the long-term thermally metamorphosed type 3 chondrites (Cody et al. 2008b), but the peak is absent in the C-XANES spectra of all the experimentally heated Tagish Lake samples. Nevertheless, the apparent lack of trends in the peak area ratio may be hidden by molecular transformation into polycyclic aromatic hydrocarbons (PAHs) that shows several resonances at the range of 285–291 eV, in addition to main π* transition at ~285 eV. For example, the 285–291 eV regions of the C-XANES spectra of benzene (which has 3 π* states) and anthracene (which has 7 π* states) are distinct from each other, as benzene has several minor peaks between 287–291 eV in addition to a prominent broad peak at ~285 eV, whereas anthracene is comparatively featureless between 287–291 eV while the main feature at ~285 eV is shown as two smaller peaks at around 284 and 286 eV respectively (Gordon et al. 2003). Therefore, while the intensity at ~287.5 eV is reduced in response to the loss of aliphatic carbon in response to heating, heating also simultaneously increases the size of polycyclic aromatic domains (increasing the number of π* states) that show different resonances across the 285–291 eV region of the C-XANES spectrum, which could then lead to a non-systematic variation in the peak area ratio.

3.3 Heating experiments – changes in the amino acid content

The procedural-blank-subtracted amino acid contents of the 6 M HCl-vapor hydrolyzed, hot-water extracts from the unheated and experimentally heated Tagish Lake meteorite samples show peaks that were identified by comparison with amino acid standards, fluorescence, retention time, and mass (Figure 7 and Table 1). The total amino acid abundance (free + bound) of the identified amino acids in the unheated Tagish Lake sample was about 89 parts-per-billion (ppb), which is consistent with the low amino acid abundance observed for the aqueously-altered

lithology of the Tagish Lake sample (sample 11i, 40–100 ppb) and other TMCCs (e.g. Y-980115 ~300 ppb) in the literature (Burton et al. 2014; Chan et al. 2016a; Glavin et al. 2012; Herd et al. 2011; Kminek et al. 2002; Pizzarello et al. 2001). The relative amino acid abundance (normalized to glycine) of the unheated Tagish Lake sample is also comparable to the aqueously-altered lithology of Tagish Lake (Figure 7).

It is often assumed that the abundance in the aliphatic moieties, including the amino acid content, would be significantly reduced by decarboxylation or conversion into aromatic C upon pyrolysis. Amino acids can be decomposed at temperatures as low as 100°C (Pietrucci et al. 2018), while proteic-amino acids are typically more thermodynamically unstable than non-proteic amino acids (e.g. β-alanine, γ-aminobutyric acid [γ-ABA]) (Kitadai 2016). Therefore, heating up to 600–900°C is expected to destroy amino acids through processes such as decarboxylation, deamination and chain homolysis which can result in the formation of a variety of simple volatile organic compounds such as amines, carboxylic acids and hydrocarbons (e.g., Bada et al. 1995; Pietrucci et al. 2018; Ratcliff et al. 1974). While the relative amino acid abundances are similar between the unheated and heated Tagish Lake meteorite samples (Figure 7), the total (identified) amino acid abundances of the heating experiment product increased by nearly tenfold from ~89 ppb in the unheated sample to ~760 ppb in the sample heated to 900°C for 96h. The total abundances of the non-protein forming D-amino acids also increased by a factor of 4–5 in the 900°C experiments. These results are completely unexpected as any amino acid present in the samples are susceptible to thermal decomposition at high temperatures. One possibility of the increase in the amino acid abundance subsequent to heating, is that amino acids are formed from simple precursor molecules such as CO, N_2 and H_2 which serve as feedstock for mineral-catalyzed Fischer Tropsch-type (FTT) reactions (e.g., Anders et al. 1973; Pizzarello 2012; Yoshino et al. 1971). The FTT reactions lead to the formation of primarily straight-chain amino acids (e.g. glycine, β-alanine, γ-ABA, ε-amino-*n*-caproic acid [EACA]) of which the amino group is on the carbon farthest from the carboxylic acid. However, when heated to 900°C, the minerals commonly associated with FTT reactions such as montmorillonite clay and magnetite are at expense to form anhydrous silicates, metal and troilite in the Tagish Lake samples (Figure 2). Although metals can also act as FTT reactions catalysts (Dry 2002), hydrogenation of CO to hydrocarbons is a very

slow process in the absence of a suitable catalyst (Hayatsu and Anders 1981; Lancet and Anders 1970). The mineral phases of which the formation thresholds are above ~350–400K, such as olivine, Fe and FeS, are not effective catalysts for the FTT reactions, whereas the phases formed at lower temperatures (e.g. montmorillonite clay and magnetite) are. This elucidates a higher abundance of organic compounds in meteorites containing these mineral phases. Therefore, the formation of amino acids via the FTT reactions in the absence of these effective catalysts should be hindered rather than enhanced. When focusing on the yield of the four-carbon amino acids ABA, the abundances of the straight-chain γ-ABA are not always higher than that of the branched isomers in the heated samples (Figure 7), which again testify against the production of amino acids via the FTT reactions. The amino acid contents were hampered by the enrichment in the L-enantiomers (e.g. the L-enantiomeric excesses (L_{ee}) of aspartic acid in the unheated Tagish Lake sample = –1.3% and 900°C 96h experiment product = 36.9%), and thus the other cause for the apparent increase in the amino acid abundance is that the amino acids were potentially terrestrial contaminants, possibly introduced via additional sample handling during the heating experiments. Even though the aqueously-altered Tagish Lake sample is commonly known to exhibit a large L_{ee} of ~45 to 99% for the proteic amino acids threonine, serine, aspartic and glutamic acids (Glavin et al. 2012), it is difficult to completely eliminate the possibility of a contribution from terrestrial contamination for this work, in particular when compound-specific isotopic analysis was implausible due to the low amino acid abundance in this lithology. In addition, Glavin et al. (2012) observed a racemic ratio for the indigenous alanine in the Tagish Lake meteorite, and yet the alanine in the experiments exhibits L_{ee}. Therefore, the carbonate-poor lithology of the Tagish Lake meteorite in this study corresponds to the aqueously-altered counterparts with very low amino acid abundance, and a confident interpretation of the change in the amino acid content upon heating is challenging at present. Therefore, we direct our focus onto the insoluble macromolecular material in the Tagish Lake meteorite.

4 DISCUSSION

4.1 IOM in the unheated Tagish Lake sample

The high abundance of aromatic material in the aqueously-altered lithology of the unheated (without being treated with experimental heating) Tagish Lake meteorite sample is clearly reflected in the C-XANES spectra, unbiased by the OM heterogeneity in the samples (Figure 5a). The IOM in the Tagish Lake meteorite has the highest aromaticity among all analyzed C1-2 chondrites (Alexander et al. 2014; Cody and Alexander 2005), and is associated with elevated δD values (Pizzarello et al. 2001) which could be indicative of aromatization processes that have converted aliphatic components into aromatic C, or an interstellar origin derived from PAHs that are ubiquitous in interstellar gas (Allamandola et al. 1987). The enhanced aromaticity in the more aqueously-altered lithology of the Tagish Lake meteorite is consistent with the observed reduction in the abundance of sp^3 C including aliphatic (CH_n, e.g. methyl, methylene, and methane) and oxygenated (CH_nO, e.g. alcohol and ether) moieties, H/C ratio, and δD values correlated to the petrologic evidences of increasing aqueous alteration (Alexander et al. 2014; Herd et al. 2011). These suggest that the conversion of aromatic C from aliphatic C during dehydration is a more probable explanation for the high aromaticity nature of the Tagish Lake OM.

The IOM in the least aqueously-altered lithology of the Tagish Lake meteorite is more comparable to the primitive, CI-, CM- and CR-like IOM with a higher aliphatic content, while that in the more aqueously-altered lithology has a lower aliphatic but higher aromatic contents and thus resembles that of the mildly heated CM, CV and CO chondrites (Alexander et al. 2014; Cody and Alexander 2005). In this study, the Tagish Lake meteorite sample exhibits a high abundance of hydrous inorganic materials (e.g., phyllosilicates), a low aliphatic organic content (Figure 5a) and amino acid abundance (Table 1), which corresponds to the most extensively aqueously altered Tagish Lake lithology (e.g., Alexander et al. 2014; Glavin et al. 2012; Herd et al. 2011; Pizzarello et al. 2001; Zolensky et al. 2002). Raman spectroscopy indicates that the IOM in the Tagish Lake meteorite is composed predominantly of highly-disordered C (Figure 3). While the Raman parameters of the IOM show affinity to that of the primitive meteorites and clearly deviate from that of

the heavily heated CV and CO chondrites, we can appreciate a uniqueness in the Tagish Lake OM as its D band parameters and I_D/I_G values do not strictly overlap with those of the other primitive meteorites, but rather occur in regions which indicate a higher disordered nature (Figure 3). (Matrajt et al. 2004) suggested a similarity between the Raman spectra of the OM in the Tagish Lake meteorite and chondritic interplanetary dust particles (IDPs). Although the OM in the unheated Tagish Lake meteorite in our study is also shown to be highly primitive in nature, its C-XANES and Raman spectra are distinct from those obtained for IDPs. The C-XANES spectra of IDPs have a large absorption of aromatic, ketone and carbonyl C (e.g., Feser et al. 2003; Flynn et al. 2003; Keller et al. 2004). A substantial fraction of the IDP OM is O substituted, and its carbonyl to aromatic C area ratio is higher than that of the Tagish Lake OM (Figure 5), which suggests a higher thermal/aqueous processing in the latter. The Raman C Γ_G value of the Tagish Lake OM is significantly lower than that of IDP OM (Figure 3c,d) (Chan et al. 2017a). The more comparable Γ_G values between the heated Tagish Lake and IDP OM are consistent with their higher O contents compared to the unheated Tagish Lake OM.

The dehydration process experienced by the Tagish Lake meteorite was distinctive from long-term parent body metamorphism since graphitization did not take place, as suggested by the absence of the 1s–σ* exciton peak in the C-XANES spectra that would indicate highly conjugated sp^2 bonded C domains (graphene structure) (Cody et al. 2008b). Despite the aqueous alteration-induced heating and dehydration processes of the parent body, the heating regime would still be considered to have occurred at "low temperatures" (<300°C) as no significant C loss has been observed, in contrast to most hydrothermally-altered chondritic samples (Yabuta et al. 2007). There is also a small contribution from the oxygenated components as shown by the weak peaks around 288.5 eV in the C-XANES spectra (Figure 5a) which indicates a minor contribution of carboxyl (O–C=O) moieties. The contribution from these oxygenated moieties indicates the onset of a late-stage oxidization process associated with the aqueous event, which echoes with the high abundance of magnetite framboids and plaquettes in the Tagish Lake meteorite which were formed via oxidation of sulfides (Zolensky et al. 2002). The consumption of O in forming the oxides has clearly removed a significant amount of O from the alteration fluid and limited the extent of oxidation of the organic phases.

Although the IOM has experienced a certain extent of heating associated with the dehydration process, the plotted Raman parameters of the aqueously altered lithology of the Tagish Lake meteorite are closer to the region of highly primitive (unheated) meteorites (CMs/CRs) and clearly deviate from that of CV and CO chondrites (Figure 3). This is because (1) the heating event was associated with a shorter-term (<10 million years [Ma]), late-stage, low temperature (<300°C) aqueous alteration where water acted as a thermal buffer that substituted long-term (>100 Ma), high temperature (400–950°C) parent body thermal metamorphism (e.g., Fujiya et al. 2013; Grimm and McSween 1989; Keil 2000), (2) the aqueous event occurred at lower temperatures, as no significant C loss was associated with the heavily-altered lithology (Yabuta et al. 2007), and (3) the Tagish Lake IOM precursor material has a highly primitive nature so that heating induced by short-term aqueous alteration did not extensively anneal the OM. Although primitive OM tends to be susceptible to heating, heating on a short-term basis does not have the required energy to fully transform the highly primitive into highly mature organics.

On the basis of these observations, it is reasonable to conclude that the starting IOM in the Tagish Lake sample prior to the heating experiments was composed of predominantly aromatic structures with a small contribution of short- and highly-branched aliphatic hydrocarbons and oxidized sp^2 bonded carbon, such as carboxyls and ketones (Figure 5). NMR spectra reveal that the CO moieties (–COOR and C=O) of the OM in the aqueously-altered Tagish Lake meteorite are not protonated, and therefore the CO groups are ketones and not aldehydes (Cody and Alexander 2005).

4.2 Influence of short-term heating on Raman spectral features

The most prominent change observed for the Raman spectrum feature in response to short-term heating is the reduction in the overall spectrum intensity. In fact, the intensity of the Raman signal does not always reflect the OM content as it can also be influenced by many other parameters, such as the focus of the laser. Nevertheless, a very consistent trend has been observed for the heated samples as they all exhibit lower Raman intensity and fluorescence background than the unheated counterpart (Figure S5). A similar effect of heating on the fluorescence background has been observed for the thermally-altered CM chondrites, which suggests that the background can be influenced by the size, distribution and concentration of OM

within the sample matrix (e.g., Quirico et al. 2014). Laser-induced fluorescence related to OM has been attributed to the presence of heteroatoms (e.g. N, O, and S) of conjugated C bonds and aliphatic components (Busemann et al. 2007; Caro et al. 2006; Matrajt et al. 2004), and can be correlated to the reduction in the bulk C content and IOM H/C ratios (Alexander et al. 2007; Alexander et al. 2013). Nevertheless, the abundance of heteroatoms in the Tagish Lake IOM is lower than that of IDPs, as suggested by the less prominent ~286.5 eV feature which can be assigned to ketones (C=O), nitrile (C≡N) and/or nitrogen heterocycles (C–N=C) in the unheated Tagish Lake sample (e.g., Cody et al. 2008a; Yabuta et al. 2014) (Figure 5).

The reduction in the fluorescence background in the heated Tagish Lake sample corresponds to the decarboxylation and dehydrogenation of the aliphatic OM (despite its small abundance) in the meteorite, as the OM in the heated Tagish Lake meteorite gains maturity through thermal annealing by losing hydrogen and heteroatoms (i.e. the hydrogenated amorphous carbons (a-C:H) fraction) to form polyaromatic structures, leads to an increase in the C=C aromatic abundance and reduction in the aliphatic content. Therefore, the H/C ratio of IOM is commonly used as an indicator of the degree of heating in the thermally-altered carbonaceous chondrites (Alexander et al. 2007; Naraoka et al. 2004). Heating of the hydrated Tagish Lake sample results in the dehydration of the hydrous minerals (principally saponite and serpentine) for which the released O could further oxidize the OM, while further dehydrogenation could lead to the development of polycondensed aromatic structures, and ultimately a reduction in the overall organic C content through oxidative conversion of IOM to CO_2.

While the Raman data indicate that the OM in the heated Tagish Lake meteorite has experienced thermal annealing by losing hydrogen and heteroatoms to form polyaromatic structures, the C-XANES data do not exhibit such a consistent trend between the samples that were subsampled and analyzed on different days. While the C-XANES data are significantly affected by sample heterogeneity, the spread of the Raman data (represented by the 1σ standard deviation of the mean, n=11–38) suggests that the trend of the heating effect is significant and not hindered by sample heterogeneity. The theoretical analytical spot size of Raman analysis (~1 μm) is much larger than that of C-XANES (~30 nm) and is therefore representative of

the overall organic structure and is less influenced by the OM heterogeneity at the smaller scale.

The D band parameters show a clear trend between the OM structure and the heating temperature (Figure 3a). The D band corresponds to the breathing modes in rings, which is attributed to the A_{1g} mode, and is inherent in the graphite lattice. It becomes observable when symmetry is broken by a crystallite edge (i.e. in-plane defects). Therefore, the D band is not present in perfectly-stacked graphite or OM without aromatic structure (Ferrari and Robertson 2004; Wang et al. 1990), and thus the D band parameters are strong tracers of the maturity of OM that are directly correlated to the presence of defects. The Γ_D value is a function of the distribution of the sizes of crystalline domains, therefore as the Tagish Lake meteorite is heated, the annealed OM is dominated by larger crystalline domains, which leads to a narrower D band width due to reduced defects. The I_D/I_G ratio increases with heating (Figure 3b), which indicates that graphitization has not been completed, as large-scale graphitization would have significantly reduced I_D/I_G (Ferrari and Robertson 2000). Despite the reduction in the heteroatoms and aliphatic contents, the OM is still present as amorphous C and not graphitized. The rapid changes in the D band parameters and the I_D/I_G ratio in response to heating up to 900°C, and the insignificant variation between the 1h and 96h experiments suggest that the IOM maturation gradient strongly depends on the time/temperature history, and that the Raman C parameters are sensitive to short-term heating. Our observation agrees with Cody et al. (2008b) in that the kinetics could be described by a log-linear behavior in response to a rapid pyrolytic reaction.

Our experimental data also indicate that the heating experiments have led to significant widening of Γ_G, and that the Γ_G value first increases and then decreases. However, this trend runs counter to that for typical meteoritic organics, where decreasing Γ_G is associated with increasing metamorphism (e.g., Busemann et al. 2007) (Figure 3c,d). Although a decrease in Γ_G (7–10 cm^{-1}) was associated with samples that were exposed to a longer heating duration (96h), the Γ_G values are still at least 14 cm^{-1} wider than the unheated samples. The challenge with Raman analysis is that there is no clear functional group level correlation with Raman parameters, unlike XANES analysis which can directly attribute the absorption features to a certain chemical moieties. Therefore, the present data underscore the fact that the trend

observed for different Raman parameters of chondritic IOM is not rigorously tied to one specific molecular structural characteristic.

Despite the complicated influences of varying molecular structures to the Raman parameters, we can appreciate that a certain structural variation can lead to the development of several trends. One confident link is that higher degrees of crystallinity (ordering) favor the development of sharper bands. The G band is attributed to the second E_{2g2} double degenerate in-plane vibration modes, which corresponds to the C–C stretching vibration. Complete graphitic ordering into a perfectly-stacked graphite results in a sharp narrow G band that corresponds to the sp^2 carbons of the graphene network, with the non-bonding π-orbitals only giving rise to weak Van der Waals forces with minimal influences to the parallel carbon layers. Therefore, a prolonged heating event, such as long-term parent body metamorphism, could lead to a reduction in Γ_G via graphitic ordering, which could ultimately result in very low Γ_G values once graphitization is complete. As a result, given that the OM structure is well characterized, such as by determining the OM graphitization extent and the abundances of oxygenated moieties, the Γ_G values can be used to distinguish between short-term heating and conventional thermal metamorphism.

Our heating experiments provide a clear explanation for the Γ_G values observed for TMCCs – their OM maturation does not strictly follow the general trend observed for meteoritic IOM. For instance, with a clear dehydration history indicated by the D band parameters, the G band parameter of the heated (≥700°C) TMCC Y-86720 plots in the zone of primitive meteorites (Busemann et al. 2007; Quirico et al. 2014), which required an extensive but brief heating episode following aqueous alteration. The ω_D (1349 cm^{-1}) and Γ_D (245 cm^{-1}) of Y-86720 (Busemann et al. 2007) would place it between the 600° and 900°C experiments on the ω_D *vs* Γ_D plot of experimentally-heated Tagish Lake (Figure 3a). Other than the disparity between the natures of the OM precursors, the difference between the trends observed for the G band parameters of the OM heated under laboratory and natural processes elucidates variations in their heating conditions, such as the abovementioned heating kinetics and confining pressure. IOM metamorphosed naturally at depth on a chondritic parent body up to kms in radius is exposed to an overburden pressure that is significantly higher than that of our heating experiments (Asphaug et al. 2002). High pressure can enhance the thermal transformation of organic C by reducing the temperature of

graphite formation and accelerating the graphitization process, leading to the formation of graphite through gradual loss of hydrogen and other heteroatoms and annealing of structural defects (Davydov et al. 2004). This justifies that short duration heating at atmospheric pressure is not as favorable for the onset of OM graphitization as metamorphism under high confining pressure.

4.3 Absence of high order graphitic component despite heating at elevated temperatures

Fourier transform infrared (FTIR) spectroscopic analysis indicated that the OM in the Tagish Lake meteorite has a significant contribution from long aliphatic chains (higher CH_2/CH_3 abundance ratio) compared to other primitive meteorites (Matrajt et al. 2004; Nakamura et al. 2002; Quirico et al. 2014), with a high aromatic to aliphatic intensity ratio (Alexander et al. 2014; Kebukawa et al. 2011). Raman, C-XANES and nuclear magnetic resonance (NMR) analyses suggested a dominant aromatic constituent (Busemann et al. 2007; Cody and Alexander 2005; Matrajt et al. 2004; Pizzarello et al. 2001; Quirico et al. 2014).

No appreciable change in the aliphatic (CH_n at ~287.5 eV) moieties was observed after the Tagish Lake meteorite samples were treated with experimental heating. Note that aliphatic moieties are present in the Tagish Lake meteorite at a small abundance and are susceptible to heating. As the aqueously-altered lithology of the Tagish Lake meteorite has a small initial abundance of aliphatic hydrocarbons, any further change to the aliphatic material in response to heating would be unrecognizable. The aromatic moieties were progressively enriched by the loss of the CO (and/or CH_n) moieties. Cleavage of hydrocarbon at elevated temperatures via decomposition of CO intermediaries can form organic acids through partial oxidation, which likely elucidates the high abundance of mono- and dicarboxylic acid content in the Tagish Lake meteorite (Pizzarello et al. 2001). Further loss of aliphatic hydrocarbon and carboxylic acids under prolonged heating would lead to total oxidation, carboxylation, and decarboxylation of the hydrocarbon skeleton into CO_2.

While C-XANES analysis of the experimentally-heated Tagish Lake is influenced by sample heterogeneity (Figure 5), our Raman data suggest that the OM in the heated Tagish Lake meteorite samples exhibits lower Raman intensity and fluorescence background, indicating the formation of polyaromatic structures by the

loss of hydrogen and heteroatoms (Figure 3). The widening of Γ_G in the experimentally heated samples indicate an increase development in the sizes of crystalline domains but graphitic ordering did not take place which would otherwise have reduced the Γ_G value. This interpretation is consistent with the C-XANES observation due to the absence of the graphene structure (~291.6 eV) that corresponds to a 1s−σ* exciton in the heated samples (Cody et al. 2008b). Although Cody et al. (2008b) observed a good correlation between the intensity of the 1s−σ* exciton and Raman spectra parameter, the C-XANES data of the experimentally heated IOM samples were compared with previously published Raman data (Γ_D and Γ_G) of chondritic IOM (Busemann et al. 2007). Therefore it could be possible that by comparing both the C-XANES and Raman data of the same laboratory heated IOM would give the same trend we observed in this study.

As noted by Cody et al. (2008b), Murchison IOM samples flash heated for up to two seconds at 600°, 1000°, and 1400°C in helium, and up to six hours at 600°, 800° and 1000°C in argon, all exhibited a systematic increase in the intensity of the 1s−σ* exciton at ~291.6 eV. In addition to the sharp peak around 291.6 eV, a pronounced broader peak at ~292.3 eV and graphene-like oscillations spanning out to 390 eV in extended X-Ray absorption fine structure (EXAFS) are also indicative of the development of graphene when studying with X-ray absorption spectroscopy (XAS) (G. Cody, personal communication, 2018). Although our Tagish Lake meteorite samples were heated to temperatures and durations comparable to those outlined in the experiments conducted by Cody et al. (2008b), the C-XANES spectra of the heated Tagish Lake samples showed that OM alteration was not accompanied by the development of the 1s−σ* exciton and the OM did not transform into highly-conjugated sp^2 bonded carbon domains as was clearly shown in the case of Murchison IOM (Cody et al. 2008b) (Figure 5). This observation agrees with the Raman spectral features: parent body metamorphism leads to the reduction in Γ_G via graphitic ordering of the OM in the chondritic meteorites, however short-term heating leads to the widening of Γ_G of the OM in the Tagish Lake meteorite, probably by increasing the abundance of carboxyl moieties, but not graphitic ordering (Figure 3d). The C=O stretching vibration for carboxylic acids has a strong Raman band at 1640–1685 cm^{-1} (Socrates 2001). Therefore, the presence of carboxylic acids would have widened the Γ_G of the OM in the heated Tagish Lake samples.

We discuss here the two possible explanations for the Tagish Lake IOM to behave so differently than Murchison IOM. First, the capacity for the highly altered and aromatic-rich IOM in the Tagish Lake sample (comparable to Tagish Lake specimens 11v and 11i) to further transform into graphene like material is limited as there is a lack of aliphatic C to begin with (Figure 5 and Figure 6). Second, while the Tagish Lake IOM is composed predominately of aromatic material, its solvent soluble organic matter (SOM) is dominated by carboxyl and dicarboxyl compounds and a low amino acid abundance (Pizzarello et al. 2001). In contrast, the IOM of Murchison is composed of both aromatic and aliphatic components, but it is more enriched in amino compounds in the soluble fraction (Martins et al. 2006; Pizzarello et al. 2001). Therefore, heating of the OM in the Tagish Lake meteorite significantly enhances the formation of oxygenated moieties, while heating of OM in the Murchison meteorite mainly reduces the abundance of the aliphatic components. With a lower O/C content in Murchison, the total loss of the aliphatic components and their conversion into aromatics far exceeds the formation of carbonyl, which is accompanied by the loss of electrons as H_2 (Alexander et al. 2014). Extensive dehydrogenation induces ordering of the aromatic moieties, leading to the development of the 1s–σ* exciton in the heated Murchison sample observed by C-XANES (Cody et al. 2008b) .

4.4 Implications for upcoming missions visiting C-complex asteroids

Small bodies are often loosely bound rubble-pile objects that were disrupted into fragments before being re-accreted, and further compacted by subsequent impact events (Okada et al. 2017b). One of the main rationales for the landing site selection of the Hayabusa2 mission is to determine the presence of hydrated minerals by measuring the 3 μm absorption feature with the near-IR spectrometer (NIRS3) (1.8–3.2 μm) (Iwata et al. 2013; Okada et al. 2017a). This 3 μm feature gradually diminishes when meteorite samples were heated to 500°C and disappears at ~700°C in response to the dehydration of phyllosilicates (Miyamoto and Zolensky 1994; Zolensky et al. 1994). One of the existing visible and near-infrared (VNIR) reflectance spectra (0.5–2.5 μm) of the Cg-type (Binzel et al. 2001), near-Earth asteroid 162173 Ryugu shows an absorption feature centered ~0.7 μm ascribed to Fe^{2+}-Fe^{3+} charge transfer in iron-bearing phyllosilicates and/or hydroxylated or oxidized iron-bearing minerals (Vilas 2008). However, the 0.7 μm feature is evident

only in this occurrence, while the heating experiment indicated that this feature disappears when Murchison was heated >400°C (Hiroi et al. 1994; Zolensky et al. 1994). Mid-IR spectra (5–25 μm) of Ryugu have a weak feature in the 11.4–12.5 μm region (McAdam et al. 2015) that can be attributed to absorption bands seen from olivine in TMCCs which indicates dehydration and dehydroxylation of phyllosilicates (King et al. 2015a). The inconsistent occurrence of the 0.7 μm phyllosilicate feature suggests that the surface of Ryugu is heterogeneous, and contains both hydrated and thermally dehydrated indigenous materials (Lazzaro et al. 2013; Vilas 2008). Such heterogeneity is a common property of main-belt C-complex asteroids (Rivkin et al. 2002), therefore it is imperative to understand the nature of organic matter and the extent of organics lost in response to thermal processing on these C-complex asteroids, which are the target asteroids of the OSIRIS-REx and Hayabusa2 sample return missions.

Understanding the mineral/organic correlation on TMCCs helps to provide guidance to the spacecraft sampling site selection in order to enhance the chances of a successful collection of the targeted organic group. The heterogeneity of Ryugu is best described by TMCCs, as they represent hydrated asteroids that were subsequently heated and dehydrated. The conditions of thermal metamorphism experienced by these meteorites are highly variable, as the heating and associated dehydration occurred *in situ* (Nakamura 2005). Thermal metamorphism, impact heating, and solar radiation have been proposed to be the possible heat sources, but short-term, high-temperature impact is a more likely pathway for the Belgica group meteorites as they appear to show no evidence of prolonged heating (Kimura and Ikeda 1992).

The chemical and bulk O isotopic compositions (Clayton and Mayeda 2001; Engrand et al. 2001; Zolensky et al. 2002) of the matrix of the carbonate-poor lithology of the Tagish Lake meteorite bears significant similarities to the TMCCs. The reflectance spectrum of the Tagish Lake meteorite resembles that observed from P- or D-type asteroids in the outer region of the main asteroid belt to a greater degree than any other meteorite (Brown et al. 2000; Hiroi et al. 2001). The D-type asteroids are expected to contain OM that did not experience any extensive heating and is more primitive than those contained in any known meteorites. The Tagish Lake meteorite has a low amino acid content (Glavin et al. 2012; Kminek et al. 2002), an extensive suite of soluble OM that includes mono- and dicarboxylic acids, pyridine carboxylic

acids and both aliphatic and aromatic hydrocarbons (Pizzarello et al. 2001). Its IOM is enriched in D and ^{15}N, and composed of predominantly aromatic structures with a small contribution of short- and highly-branched aliphatic hydrocarbons and oxidized sp^2 bonded carbon (Alexander et al. 2014; Herd et al. 2011; Nakamura-Messenger et al. 2006; Pizzarello et al. 2001), which are indicative of their formation at low temperatures and an origin of cold molecular clouds and the outer protosolar disk. The highly primitive and unheated nature of the Tagish Lake meteorite makes it an ideal candidate for the investigation of the effect of heating on the OM content, in contrast to other chondritic OM which have already been chemically and structurally thermally altered to various extents.

The results of our short-term heating experiments conducted on the more hydrous lithology of the Tagish Lake meteorite imply that thermal metamorphism often reduces the overall C content, particularly in the heat-sensitive SOM species. Therefore, despite the short duration (up to 96h), the post-hydration local heating of Ryugu could have significantly reduced the abundance and altered the primitive nature of the OM, which accordingly impacts the scientific objective of the sample return mission – to obtain pristine asteroidal samples that enables us to investigate the diversification of organic materials through interaction with minerals and water in a planetesimal (Tachibana et al. 2014; Watanabe et al. 2017).

The samples returned by the Hayabusa2 mission that are destined for SOM analysis, should preferably be derived from the unheated lithology. In contrast, organic analysis of the heated lithology could have been influenced by (1) dehydration of phyllosilicates, (2) hydrolysis of organics at elevated temperatures by the water released via phyllosilicate dehydration, (3) reduction in overall C and H/C contents, (4) reduction in the aliphatic component and development of the organic C into larger aromatic domains, and (5) consumption of the SOM and their incorporation into the IOM structure and evolution of the IOM isotopic composition. Nevertheless, serpentine without Fe^{3+} does not show the 0.7 μm band, and not all altered CM/CI meteorites exhibit this feature (McAdam et al. 2015). Therefore the absence of the 0.7 μm absorption feature is not strictly equivalent to a lack of aqueous alteration or the dehydration of serpentine.

Several concerns regarding the proper OM interpretation are raised here. The Raman spectroscopic features are controlled by the nature of the OM, the heating duration and temperature. Therefore, the D band parameters of the OM that was subjected to transient heating do not strictly follow the same kinetics as chondritic OM that was processed by long-term thermal metamorphism (e.g. internal heating from short-lived radionuclides). OM heated by transient, high temperature processes on hydrous C-type asteroids cannot be described by the same D band parameters as that processed by long-term heating at lower temperatures. Raman G band parameters and the graphitic exciton ~291.6 eV in C-XANES can be combined to reveal the heating kinetics. Therefore, the 291.6 eV absorption band in C-XANES spectra is a handy cosmothermometer for some chondritic IOM, but it does not offer an accurate description to the thermal alteration history of TMCCs, as the presence of abundant hydroxylated minerals (e.g. hydroxylated phyllosilicate) and organics (e.g. carboxyls, ketones) compensates for the conversion of aliphatic into aromatic components by the formation of carbonyl moieties, and thus the OM does not get fully graphitized. These account for the wider Γ_G in the Raman spectrum and the absence of the C-XANES 291.6 eV absorption band in the OM of the heated Tagish Lake meteorite samples.

5 CONCLUSIONS

We explore the effects of short-term heating on the OM in the carbonate-poor, aqueously altered lithology of the Tagish Lake meteorite with Raman spectroscopy, C-XANES and UPLC-FD/QToF-MS. OM maturity and graphitization is dependent on the nature of the OM precursor, the heating duration and temperature, therefore the Raman and C-XANES spectral features of the OM in the experimentally-heated Tagish Lake meteorite samples significantly differ from that of the chondritic OM such as that in Murchison which has a lower abundance of oxygenated moieties, and other meteorite samples which were altered by prolonged metamorphism. Typical cosmothermometers cannot be used to interpret the peak heating temperature of meteorites that were altered by transient heating processes such as impact heating and/or solar radiation. Nevertheless, the effect of short-term heating on the OM in the Tagish Lake meteorite is well demonstrated by the distinctive Raman G band width, and can be used as a guide when typical cosmothermometers cannot be applied.

ACKNOWLEDGEMENTS

We acknowledge Charley Roots and Jim Brook for the Tagish Lake sample. This study was supported by NASA's Cosmochemistry, Emerging Worlds, and Hayabusa2 Participating Scientist Programs (M.E.Z. is the PI), and the SERVII Center for Lunar Science and Exploration. Q.H.S.C. acknowledges support from the NASA Postdoctoral Program at the Johnson Space Center, administered by the Universities Space Research Association. Y.K. is supported by the Astrobiology Center Program of National Institutes of Natural Sciences (NINS) (Grant Number AB281004 and AB291005). We thank George Cody for careful reviews which helped improve the quality of this manuscript. We thank Aaron Burton for the use of UPLC-FD/QToF-MS facility. Beamline 5.3.2.2 at the ALS is supported by the Director of the Office of Science, Department of Energy under Contract No. DE-AC02-05CH11231. STXM analysis in KEK (Proposal No. 2016S2-002) was supported by Ministry of Education, Culture, Sports, Science and Technology (MEXT) Grant-in-Aid for Scientific Research (KAKENHI) (17H06458).

REFERENCES

Akai J. 1988. Incompletely transformed serpentine-type phyllosilicates in the matrix of Antarctic CM chondrites. Geochimica et Cosmochimica Acta 52(6): 1593-1599.

Alexander C. M. O. D., Fogel M. L., Yabuta H., and Cody G. D. 2007. The origin and evolution of chondrites recorded in the elemental and isotopic compositions of their macromolecular organic matter. Geochimica et Cosmochimica Acta 71: 4380-4403.

Alexander C. M. O. D., Howard K. T., Bowden R., and Fogel M. L. 2013. The classification of CM and CR chondrites using bulk H, C and N abundances and isotopic compositions. Geochimica et Cosmochimica Acta 123: 244-260.

Alexander C. M. O. D., Cody G. D., Kebukawa Y., Bowden R., Fogel M. L., Kilcoyne A. L. D., Nittler L. R., and Herd C. D. K. 2014. Elemental, isotopic, and structural changes in Tagish Lake insoluble organic matter produced by parent body processes. Meteoritics & Planetary Science 49(4): 503-525.

Allamandola L. J., Sandford S. A., and Wopenka B. 1987. Interstellar Polycyclic Aromatic Hydrocarbons and Carbon in Interplanetary Dust Particles and Meteorites. Science 237(4810): 56-59.

Anders E., Hayatsu R., and Studier M. H. 1973. Organic Compounds in Meteorites They may have formed in the solar nebula, by catalytic reactions of carbon monoxide, hydrogen, and ammonia. Science 182(4114): 781-790.

Aoya M., Kouketsu Y., Endo S., Shimizu H., Mizukami T., Nakamura D., and Wallis S. 2010. Extending the applicability of the Raman carbonaceous-material geothermometer using data from contact metamorphic rocks. Journal of Metamorphic Geology 28(9): 895-914.

Asphaug E., Ryan E. V., and Zuber M. T. 2002. Asteroid interiors. Asteroids III 1: 463-484.

Bada J. L., Miller S. L., and Zhao M. 1995. The stability of amino acids at submarine hydrothermal vent temperatures. Origins of Life and Evolution of Biospheres 25(1): 111-118.

Bernard S., Beyssac O., Benzerara K., Findling N., Tzvetkov G., and Brown Jr G. E. 2010. XANES, Raman and XRD study of anthracene-based cokes and saccharose-based chars submitted to high-temperature pyrolysis. Carbon 48(9): 2506-2516.

Beyssac O., Goffé B., Chopin C., and Rouzaud J. N. 2002. Raman spectra of carbonaceous material in metasediments: a new geothermometer. Journal of Metamorphic Geology 20(9): 859-871.

Binzel R. P., Harris A. W., Bus S. J., and Burbine T. H. 2001. Spectral Properties of Near-Earth Objects: Palomar and IRTF Results for 48 Objects Including Spacecraft Targets (9969) Braille and (10302) 1989 ML. Icarus 151(2): 139-149.

Bonal L., Quirico E., Bourot-Denise M., and Montagnac G. 2006. Determination of the petrologic type of CV3 chondrites by Raman spectroscopy of included organic matter. Geochimica et Cosmochimica Acta 70(7): 1849-1863.

Bonal L., Bourot-Denise M., Quirico E., Montagnac G., and Lewin E. 2007. Organic matter and metamorphic history of CO chondrites. Geochimica et Cosmochimica Acta 71: 1605-1623.

Brown P. G., Hildebrand A. R., Zolensky M. E., Grady M., Clayton R. N., Mayeda T. K., Tagliaferri E., Spalding R., MacRae N. D., Hoffman E. L., Mittlefehldt D. W., Wacker J. F., Bird J. A., Campbell M. D., Carpenter R., Gingerich H., Glatiotis M., Greiner E., Mazur M. J., McCausland P. J., Plotkin H., and Mazur T. R. 2000. The Fall, Recovery, Orbit, and Composition of the Tagish Lake Meteorite: A New Type of Carbonaceous Chondrite. Science 290(5490): 320-325.

Burton A. S., Grunsfeld S., Elsila J. E., Glavin D. P., and Dworkin J. P. 2014. The effects of parent-body hydrothermal heating on amino acid abundances in CI-like chondrites. Polar Science 8(3): 255-263.

Busemann H., Alexander M. O. D., and Nittler L. R. 2007. Characterization of insoluble organic matter in primitive meteorites by microRaman spectroscopy. Meteoritics & Planetary Science 42(7-8): 1387-1416.

Caro G. M. M., Matrajt G., Dartois E., Nuevo M., d'Hendecourt L., Deboffle D., Montagnac G., Chauvin N., Boukari C., and Du D. L. 2006. Nature and evolution of the dominant carbonaceous matter in interplanetary dust particles: effects of irradiation and identification with a type of amorphous carbon. A&A 459(1): 147-159.

Chan Q., Franchi I., and Wright I. 2017a Organic components in interplanetary dust particles and their implications for the synthesis of cometary organics. In *80th Annual Meeting of the Meteoritical Society 2017*, pp. 6157.

Chan Q. H. S., Chikaraishi Y., Takano Y., Ogawa N. O., and Ohkouchi N. 2016a. Amino acid compositions in heated carbonaceous chondrites and their compound-specific nitrogen isotopic ratios. Earth, Planets and Space 68(1): 7.

Chan Q. H. S., Zolensky M. E., Martinez J. E., Tsuchiyama A., and Miyake A. 2016b. Magnetite plaquettes are naturally asymmetric materials in meteorites. American Mineralogist 101(9): 2041-2050.

Chan Q. H. S., Zolensky M. E., Bodnar R. J., Farley C., and Cheung J. C. H. 2017b. Investigation of organo-carbonate associations in carbonaceous chondrites by Raman spectroscopy. Geochimica et Cosmochimica Acta 201: 392-409.

Chan Q. H. S., Zolensky M., Kebukawa Y., Fries M., Ito M., Steele A., Rahman Z., Nakato A., Kilcoyne A. L. D., Suga H., Takahashi Y., Takeichi Y., and Mase K. 2018. Organic matter in extraterrestrial water-bearing salt crystals. Science Advances 4: eaao3521.

Clayton R. and Mayeda T. 2001 Oxygen isotopic composition of the Tagish Lake carbonaceous chondrite. In *Lunar and Planetary Science Conference*.

Clayton R. N. and Mayeda T. K. 1999. Oxygen isotope studies of carbonaceous chondrites. Geochimica et Cosmochimica Acta 63(13–14): 2089-2104.

Cody G. D. and Alexander C. M. O. D. 2005. NMR studies of chemical structural variation of insoluble organic matter from different carbonaceous chondrite groups. Geochimica et Cosmochimica Acta 69(4): 1085-1097.

Cody G. D., Ade H., Alexander M. O. D., Araki T., Butterworth A., Fleckenstein H., Flynn G., Gilles M. K., Jacobsen C., Kilcoyne A. L. D., Messenger K., Sandford S. A., Tyliszczak T., Westphal A. J., Wirick S., and Yabuta H. 2008a. Quantitative organic and light-element analysis of comet 81P/Wild 2 particles using C-, N-, and O-μ-XANES. Meteoritics & Planetary Science 43(1-2): 353-365.

Cody G. D., Alexander C. M. O. D., Yabuta H., Kilcoyne A. L. D., Araki T., Ade H., Dera P., Fogel M., Militzer B., and Mysen B. O. 2008b. Organic thermometry for chondritic parent bodies. Earth and Planetary Science Letters 272(1–2): 446-455.

Davydov V. A., Rakhmanina A. V., Agafonov V., Narymbetov B., Boudou J. P., and Szwarc H. 2004. Conversion of polycyclic aromatic hydrocarbons to graphite and diamond at high pressures. Carbon 42(2): 261-269.

Derenne S. and Robert F. 2010. Model of molecular structure of the insoluble organic matter isolated from Murchison meteorite. Meteoritics & Planetary Science 45(9): 1461-1475.

Dischler B., Bubenzer A., and Koidl P. 1983. Bonding in hydrogenated hard carbon studied by optical spectroscopy. Solid State Communications 48(2): 105-108.

Dry M. E. 2002. The Fischer–Tropsch process: 1950–2000. Catalysis Today 71(3): 227-241.

Engrand C., Gounelle M., Duprat J., and Zolensky M. 2001 In-situ oxygen isotopic composition of individual minerals in Tagish Lake, a unique type 2 carbonaceous meteorite. In *Lunar and Planetary Science Conference*.

Ferrari A. C. and Robertson J. 2000. Interpretation of Raman spectra of disordered and amorphous carbon. Physical Review B 61(20): 14095-14107.

Ferrari A. C. and Robertson J. 2004. Raman spectroscopy of amorphous, nanostructured, diamond–like carbon, and nanodiamond. Philosophical Transactions of the Royal Society of London A: Mathematical, Physical and Engineering Sciences 362(1824): 2477-2512.

Feser M., Wirick S., Flynn G., and Keller L. 2003 Combined carbon, nitrogen, and oxygen XANES spectroscopy on hydrated and anhydrous interplanetary dust particles. In *Lunar and Planetary Science Conference*, pp. 1875, League City, Texas.

Flynn G. J., Keller L. P., Feser M., Wirick S., and Jacobsen C. 2003. The origin of organic matter in the solar system: evidence from the interplanetary dust particles. Geochimica et Cosmochimica Acta 67(24): 4791-4806.

Fujiya W., Sugiura N., Sano Y., and Hiyagon H. 2013. Mn–Cr ages of dolomites in CI chondrites and the Tagish Lake ungrouped carbonaceous chondrite. Earth and Planetary Science Letters 362: 130-142.

1013 Gaffey M. J., Bell J. F., and Cruikshank D. P. 1989 Reflectance spectroscopy and
1014 asteroid surface mineralogy. In *Asteroid II* (eds. R. P. Binzel, T. Gehrels, and
1015 M. S. Matthews), pp. 98-127. Univ. Arizona Press, Tucson, Arizona.

1016 Glavin D. P., Dworkin J. P., Aubrey A., Botta O., Doty III J. H., Martins Z., and Bada
1017 J. L. 2006. Amino acid analyses of Antarctic CM2 meteorites using liquid
1018 chromatography–time of flight–mass spectrometry. Meteoritics & Planetary
1019 Science 41(6): 889-902.

1020 Glavin D. P., Elsila J. E., Burton A. S., Callahan M. P., Dworkin J. P., Hilts R. W.,
1021 and Herd C. D. K. 2012. Unusual nonterrestrial l-proteinogenic amino acid
1022 excesses in the Tagish Lake meteorite. Meteoritics & Planetary Science 47(8):
1023 1347-1364.

1024 Gordon M. L., Tulumello D., Cooper G., Hitchcock A. P., Glatzel P., Mullins O. C.,
1025 Cramer S. P., and Bergmann U. 2003. Inner-Shell Excitation Spectroscopy of
1026 Fused-Ring Aromatic Molecules by Electron Energy Loss and X-ray Raman
1027 Techniques. The Journal of Physical Chemistry A 107(41): 8512-8520.

1028 Grimm R. E. and McSween H. Y. 1989. Water and the thermal evolution of
1029 carbonaceous chondrite parent bodies. Icarus 82(2): 244-280.

1030 Hayatsu R. and Anders E. 1981 Organic compounds in meteorites and their origins. In
1031 *Cosmo- and Geochemistry*, pp. 1-37. Springer Berlin Heidelberg.

1032 Herd C. D. K., Blinova A., Simkus D. N., Huang Y., Tarozo R., Alexander C. M. O.
1033 D., Gyngard F., Nittler L. R., Cody G. D., Fogel M. L., Kebukawa Y.,
1034 Kilcoyne A. L. D., Hilts R. W., Slater G. F., Glavin D. P., Dworkin J. P.,
1035 Callahan M. P., Elsila J. E., De Gregorio B. T., and Stroud R. M. 2011. Origin
1036 and Evolution of Prebiotic Organic Matter As Inferred from the Tagish Lake
1037 Meteorite. Science 332(6035): 1304-1307.

1038 Hiroi T., Pieters C. M., Zolensky M. E., and Lipschutz M. E. 1993. Evidence of
1039 Thermal Metamorphism on the C, G, B, and F Asteroids. Science 261(5124):
1040 1016-1018.

1041 Hiroi T., Peters C., Zolensky M. E., and Lipschutz P. 1994. Possible thermal
1042 metamorphism of the C, G, B, and F asteroids detected from their reflectance
1043 spectra in comparison with carbonaceous chondrites. Proc. NIPR Symp.
1044 Antarctic Meteor. 7(

1045 Hiroi T., Zolensky M. E., Pieters C. M., and Lipschutz M. E. 1996. Thermal
1046 metamorphism of the C, G, B, and F asteroids seen from the 0.7 μm, 3 μm,
1047 and UV absorption strengths in comparison with carbonaceous chondrites.
1048 Meteoritics & Planetary Science 31(3): 321-327.

1049 Hiroi T., Zolensky M. E., and Pieters C. M. 2001. The Tagish Lake Meteorite: A
1050 Possible Sample from a D-Type Asteroid. Science 293(5538): 2234-2236.

1051 Homma Y., Kouketsu Y., Kagi H., Mikouchi T., and Yabuta H. 2015. Raman
1052 spectroscopic thermometry of carbonaceous material in chondrites: four–band
1053 fitting analysis and expansion of lower temperature limit. Journal of
1054 Mineralogical and Petrological Sciences 110(6): 276-282.

1055 Ikeda Y. 1991. Petrology and mineralogy of the Yamato-82162 chondrite (CI). Proc.
1056 NIPR Symp. Antarctic Meteor. 4(

Ikeda Y. 1992. An overview of the research consortium, "Antarctic carbonaceous chondrites with CI affinities, Yamato-86720, Yamato-82162 and Belgica-7904". Proc. NIPR Symp. Antarctic Meteor. 5(

Iwata T., Kitazato K., Abe M., Ohtake M., Matsuura S., Tsumura K., Hirata N., Honda C., Takagi Y., and Nakauchi Y. 2013 Results of the critical design for nirs3: the near infrared spectrometer on Hayabusa-2. In *Lunar and Planetary Science Conference*, pp. 1908.

Kebukawa Y., Alexander C. M. O. D., and Cody G. D. 2011. Compositional diversity in insoluble organic matter in type 1, 2 and 3 chondrites as detected by infrared spectroscopy. Geochimica et Cosmochimica Acta 75(12): 3530-3541.

Kebukawa Y., Zolensky M. E., Chan Q. H. S., Nagao K., Kilcoyne A. L. D., Bodnar R. J., Farley C., Rahman Z., Le L., and Cody G. D. 2017. Characterization of carbonaceous matter in xenolithic clasts from the Sharps (H3.4) meteorite: Constraints on the origin and thermal processing. Geochimica et Cosmochimica Acta 196: 74-101.

Keil K. 2000. Thermal alteration of asteroids: evidence from meteorites. Planetary and Space Science 48(10): 887-903.

Keller L. P., Messenger S., Flynn G. J., Clemett S., Wirick S., and Jacobsen C. 2004. The nature of molecular cloud material in interplanetary dust. Geochimica et Cosmochimica Acta 68(11): 2577-2589.

Kilcoyne A. L. D., Tyliszczak T., Steele W. F., Fakra S., Hitchcock P., Franck K., Anderson E., Harteneck B., Rightor E. G., Mitchell G. E., Hitchcock A. P., Yang L., Warwick T., and Ade H. 2003. Interferometer-controlled scanning transmission X-ray microscopes at the Advanced Light Source. Journal of Synchrotron Radiation 10(2): 125-136.

Kimura M. and Ikeda Y. 1992. Mineralogy and petrology of an unusual Belgica-7904 carbonaceous chondrites: genetic relationships among the components. Proc. NIPR Symp. Antarctic Meteor. 5(

King A., Solomon J., Schofield P., and Russell S. 2015a. Characterising the CI and CI-like carbonaceous chondrites using thermogravimetric analysis and infrared spectroscopy. Earth, Planets and Space 67(1): 1-12.

King A. J., Schofield P. F., Howard K. T., and Russell S. S. 2015b. Modal mineralogy of CI and CI-like chondrites by X-ray diffraction. Geochimica et Cosmochimica Acta 165: 148-160.

Kitadai N. 2016. Predicting Thermodynamic Behaviors of Non-Protein Amino Acids as a Function of Temperature and pH. Origins of Life and Evolution of Biospheres 46(1): 3-18.

Kminek G., Botta O., Glavin D. P., and Bada J. L. 2002. Amino acids in the Tagish Lake meteorite. Meteoritics & Planetary Science 37(5): 697-701.

Kouketsu Y., Mizukami T., Mori H., Endo S., Aoya M., Hara H., Nakamura D., and Wallis S. 2014. A new approach to develop the Raman carbonaceous material geothermometer for low-grade metamorphism using peak width. Island Arc 23(1): 33-50.

Lancet M. S. and Anders E. 1970. Carbon Isotope Fractionation in the Fischer-Tropsch Synthesis and in Meteorites. Science 170(3961): 980-982.

Lazzaro D., Barucci M. A., Perna D., Jasmim F. L., Yoshikawa M., and Carvano J. M. F. 2013. Rotational spectra of (162173) 1999 JU3, the target of the Hayabusa2 mission. Astronomy & Astrophysics 549: L2.

Le Guillou C., Bernard S., Brearley A. J., and Remusat L. 2014. Evolution of organic matter in Orgueil, Murchison and Renazzo during parent body aqueous alteration: In situ investigations. Geochimica et Cosmochimica Acta 131: 368-392.

Lessard R., Cuny J., Cooper G., and Hitchcock A. P. 2007. Inner-shell excitation of gas phase carbonates and α,γ-dicarbonyl compounds. Chemical Physics 331(2): 289-303.

Martins Z., Watson J. S., Sephton M. A., Botta O., Ehrenfreund P., and Gilmour I. 2006. Free dicarboxylic and aromatic acids in the carbonaceous chondrites Murchison and Orgueil. Meteoritics & Planetary Science 41(7): 1073-1080.

Matrajt G., Borg J., Raynal P. I., Djouadi Z., d'Hendecourt L., Flynn G., and Deboffle D. 2004. FTIR and Raman analyses of the Tagish Lake meteorite: Relationship with the aliphatic hydrocarbons observed in the Diffuse Interstellar Medium. A&A 416(3): 983-990.

McAdam M. M., Sunshine J. M., Howard K. T., and McCoy T. M. 2015. Aqueous alteration on asteroids: Linking the mineralogy and spectroscopy of CM and CI chondrites. Icarus 245: 320-332.

Miyamoto M. and Zolensky M. E. 1994. Infrared diffuse reflectance spectra of carbonaceous chondrites: Amount of hydrous minerals. Meteoritics 29(6): 849-853.

Nakamura-Messenger K., Messenger S., Keller L. P., Clemett S. J., and Zolensky M. E. 2006. Organic Globules in the Tagish Lake Meteorite: Remnants of the Protosolar Disk. Science 314(5804): 1439-1442.

Nakamura K., Zolensky M. E., Tomita S., Nakashima S., and Tomeoka K. 2002. Hollow organic globules in the Tagish Lake meteorite as possible products of primitive organic reactions. International Journal of Astrobiology 1(03): 179-189.

Nakamura T. 2005. Post-hydration thermal metamorphism of carbonaceous chondrites. J. Mineral. Petrol. Sci. 100(

Nakato A., Nakamura T., Kitajima F., and Noguchi T. 2008. Evaluation of dehydration mechanism during heating of hydrous asteroids based on mineralogical and chemical analysis of naturally and experimentally heated CM chondrites. Earth, Planets and Space 60(8): 855-864.

Nakato A., Chan Q., Nakamura T., Kebukawa Y., and Zolensky M. 2016 Mineralogy of Experimentally Heated Tagish Lake. In *Lunar and Planetary Science Conference*, The Woodlands, TX; United States.

Naraoka H., Mita H., Komiya M., Yoneda S., Kojima H., and Shimoyama A. 2004. A chemical sequence of macromolecular organic matter in the CM chondrites. Meteoritics & Planetary Science 39(3): 401-406.

Okada T., Binzel R. P., Connolly H. C., Yada T., and Ohtsuki K. 2017a. Special issue "Science of solar system materials examined from Hayabusa and future missions (II)". Earth, Planets and Space 69(1): 31.

Okada T., Fukuhara T., Tanaka S., Taguchi M., Imamura T., Arai T., Senshu H., Ogawa Y., Demura H., Kitazato K., Nakamura R., Kouyama T., Sekiguchi T., Hasegawa S., Matsunaga T., Wada T., Takita J., Sakatani N., Horikawa Y., Endo K., Helbert J., Müller T. G., and Hagermann A. 2017b. Thermal Infrared Imaging Experiments of C-Type Asteroid 162173 Ryugu on Hayabusa2. Space Science Reviews 208(1): 255-286.

Pearson V. K., Sephton M. A., Franchi I. A., Gibson J. M., and Gilmour I. 2006. Carbon and nitrogen in carbonaceous chondrites: Elemental abundances and stable isotopic compositions. Meteoritics & Planetary Science 41(12): 1899-1918.

Pietrucci F., Aponte J. C., Starr R., Pérez-Villa A., Elsila J. E., Dworkin J. P., and Saitta A. M. 2018. Hydrothermal Decomposition of Amino Acids and Origins of Prebiotic Meteoritic Organic Compounds. ACS Earth and Space Chemistry.

Pizzarello S., Huang Y., Becker L., Poreda R. J., Nieman R. A., Cooper G., and Williams M. 2001. The Organic Content of the Tagish Lake Meteorite. Science 293(5538): 2236-2239.

Pizzarello S. 2012. Catalytic syntheses of amino acids and their significance for nebular and planetary chemistry. Meteoritics & Planetary Science 47(8): 1291-1296.

Quirico E., Raynal P.-I., and Bourot-Denise M. 2003. Metamorphic grade of organic matter in six unequilibrated ordinary chondrites. Meteoritics & Planetary Science 38(6): 795-811.

Quirico E., Orthous-Daunay F.-R., Beck P., Bonal L., Brunetto R., Dartois E., Pino T., Montagnac G., Rouzaud J.-N., Engrand C., and Duprat J. 2014. Origin of insoluble organic matter in type 1 and 2 chondrites: New clues, new questions. Geochimica et Cosmochimica Acta 136: 80-99.

Ratcliff M. A., Medley E. E., and Simmonds P. G. 1974. Pyrolysis of amino acids. Mechanistic considerations. The Journal of Organic Chemistry 39(11): 1481-1490.

Rivkin A., Howell E., Vilas F., and Lebofsky L. 2002. Hydrated minerals on asteroids: The astronomical record. Asteroids III 1: 235-253.

Socrates G. 2001 *Infrared and Raman Characteristic Group Frequencies: Tables and Charts*. John Wiley & Sons. pp. 347.

Tachibana S., Abe M., Arakawa M., Fujimoto M., Iijima Y., Ishiguro M., Kitazato K., Kobayashi N., Namiki N., Okada T., Okazaki R., Sawada H., Sugita S., Takano Y., Tanaka S., Watanabe S., Yoshikawa M., Kuninaka H., and The Hayabusa2 Project T. 2014. Hayabusa2: Scientific importance of samples returned from C-type near-Earth asteroid (162173) 1999 JU$_3$. Geochemical Journal 48(6): 571-587.

Takeichi Y., Inami N., Suga H., Miyamoto C., Ueno T., Mase K., Takahashi Y., and Ono K. 2016. Design and performance of a compact scanning transmission X-

ray microscope at the Photon Factory. Review of Scientific Instruments 87(1): 013704.

Tomeoka K., Kojima H., and Yanai K. 1989a. Yamato-82162: a new kind of CI carbonaceous chondrite from Antarctica. Proc. NIPR Symp. Antarctic Meteor. 2(

Tomeoka K., Kojima H., and Yanai K. 1989b. Yamato-86720: A CM carbonaceous chondrite having experienced extensive aqueous alteration and thermal metamorphism. Proc. NIPR Symp. Antarctic Meteor. 2(

Tonui E., Zolensky M., Hiroi T., Nakamura T., Lipschutz M. E., Wang M.-S., and Okudaira K. 2014. Petrographic, chemical and spectroscopic evidence for thermal metamorphism in carbonaceous chondrites I: CI and CM chondrites. Geochimica et Cosmochimica Acta 126: 284-306.

Tuinstra F. and Koenig J. L. 1970a. Characterization of Graphite Fiber Surfaces with Raman Spectroscopy. Journal of Composite Materials 4(4): 492-499.

Tuinstra F. and Koenig J. L. 1970b. Raman Spectrum of Graphite. The Journal of Chemical Physics 53(3): 1126-1130.

Vilas F. 2008. Spectral Characteristics of Hayabusa 2 Near-Earth Asteroid Targets 162173 1999 JU3 and 2001 QC34. The Astronomical Journal 135(4): 1101.

Wang Y., Alsmeyer D. C., and McCreery R. L. 1990. Raman spectroscopy of carbon materials: structural basis of observed spectra. Chemistry of Materials 2(5): 557-563.

Watanabe S.-i., Tsuda Y., Yoshikawa M., Tanaka S., Saiki T., and Nakazawa S. 2017. Hayabusa2 Mission Overview. Space Science Reviews 208(1): 3-16.

Yabuta H., Williams L. B., Cody G. D., Alexander C. M. O. D., and Pizzarello S. 2007. The insoluble carbonaceous material of CM chondrites: A possible source of discrete organic compounds under hydrothermal conditions. Meteoritics & Planetary Science 42(1): 37-48.

Yabuta H., Alexander C. M. O. D., Fogel M. L., Kilcoyne A. L. D., and Cody G. D. 2010. A molecular and isotopic study of the macromolecular organic matter of the ungrouped C2 WIS 91600 and its relationship to Tagish Lake and PCA 91008. Meteoritics & Planetary Science 45(9): 1446-1460.

Yabuta H., Uesugi M., Naraoka H., Ito M., Kilcoyne A., Sandford S., Kitajima F., Mita H., Takano Y., Yada T., Karouji Y., Ishibashi Y., Okada T., and Abe M. 2014. X-ray absorption near edge structure spectroscopic study of Hayabusa category 3 carbonaceous particles. Earth, Planets and Space 66(1): 1-8.

Yoshino D., Hayatsu K., and Anders E. 1971. Origin of organic matter in early solar system—III. Amino acids: Catalytic synthesis. Geochimica et Cosmochimica Acta 35(9): 927-938.

Zolensky M., Lipschutz M., and Hiroi T. 1994 Mineralogy of artificially heated carbonaceous chondrites. In *Lunar and Planetary Science Conference*, pp. 1567-1568.

Zolensky M. E., Nakamura K., Gounelle M., Mikouchi T., Kasama T., Tachikawa O., and Tonui E. 2002. Mineralogy of Tagish Lake: An ungrouped type 2 carbonaceous chondrite. Meteoritics & Planetary Science 37(5): 737-761.

1232

1233

1234

FIGURES AND FIGURE CAPTIONS

Figure 1. (a) 3D rendering of the Tagish Lake meteorite samples produced from XRCT. The arrow shows the area of the carbonate-poor lithology. (b) A slice image of Tagish Lake sample taken at the dashed line in (a). SE images (c,e) and EDX Ca X-ray maps (d,f) of the carbonate-rich (right) and carbonate-poor (middle) lithologies of the Tagish Lake meteorite, obtained by SEM analysis. All EDX elemental maps of the carbonate-poor lithology are shown in Figure S1.

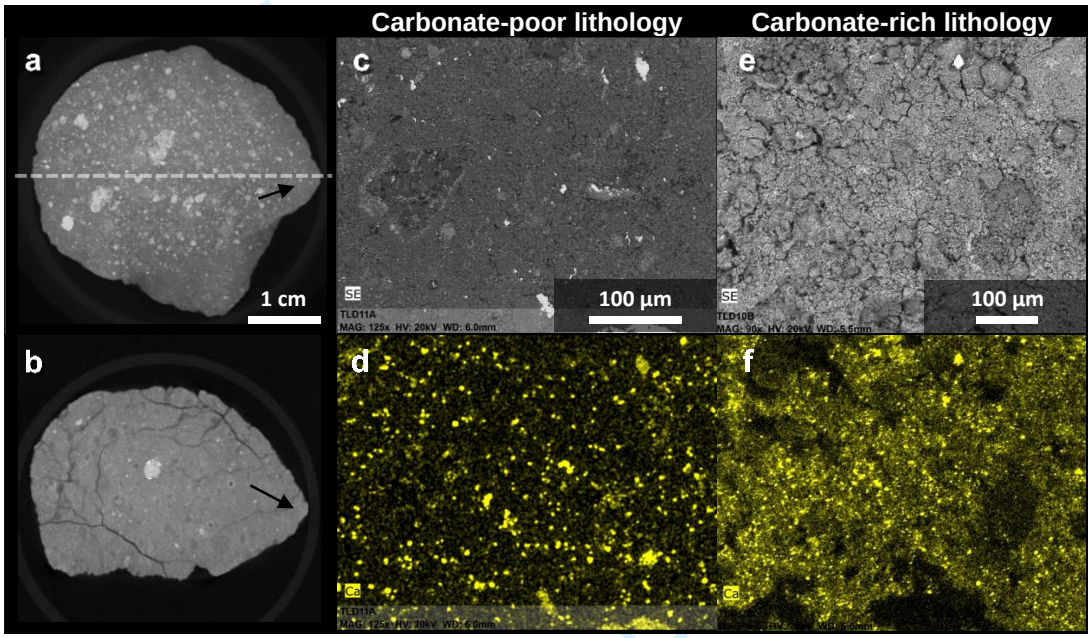

Figure 2. Optical photos of the Tagish Lake meteorite sample before and after the heating experiment at 900°C for 96h. The sample shows significant weight loss (~20%) upon heating which indicates the dehydration of phyllosilicates. Common mineral phases observed in the matrix of the unheated carbonate-poor lithology of the Tagish Lake meteorite such as phyllosilicates, magnetite and Fe-Ni sulfides were converted into anhydrous silicates, Fe-Ni metal and troilite via dehydration and reduction.

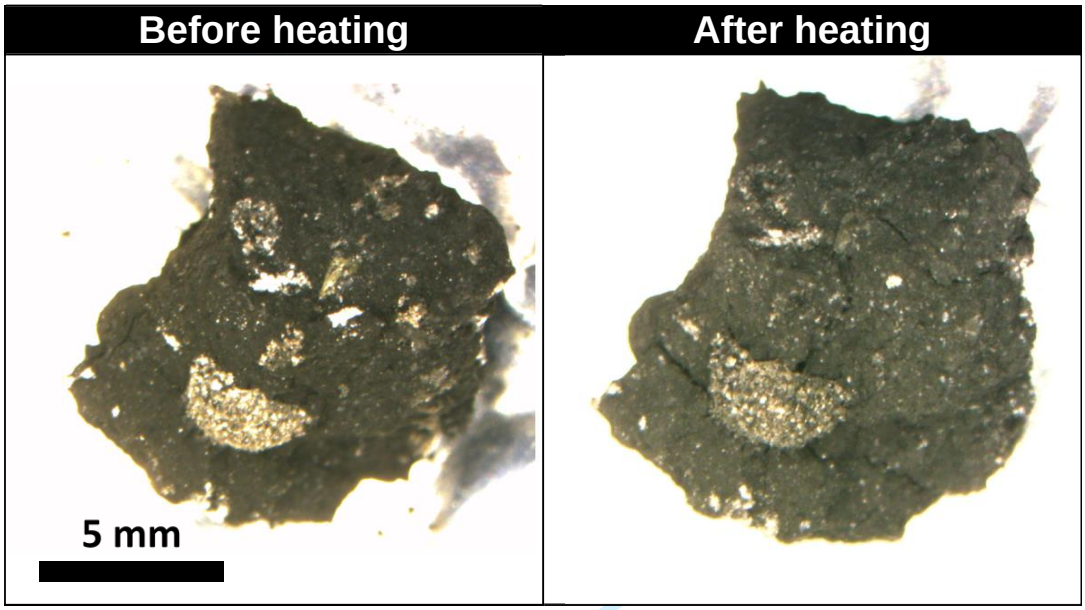

Figure 3. Comparison of the C Raman band parameters of the OM in the heating-experimental products of the Tagish Lake meteorite to the OM in chondrites and IDPs. Data of the chondrites and IDPs were obtained from Chan et al. (2017a). Uncertainties are 1σ standard deviation of the mean.

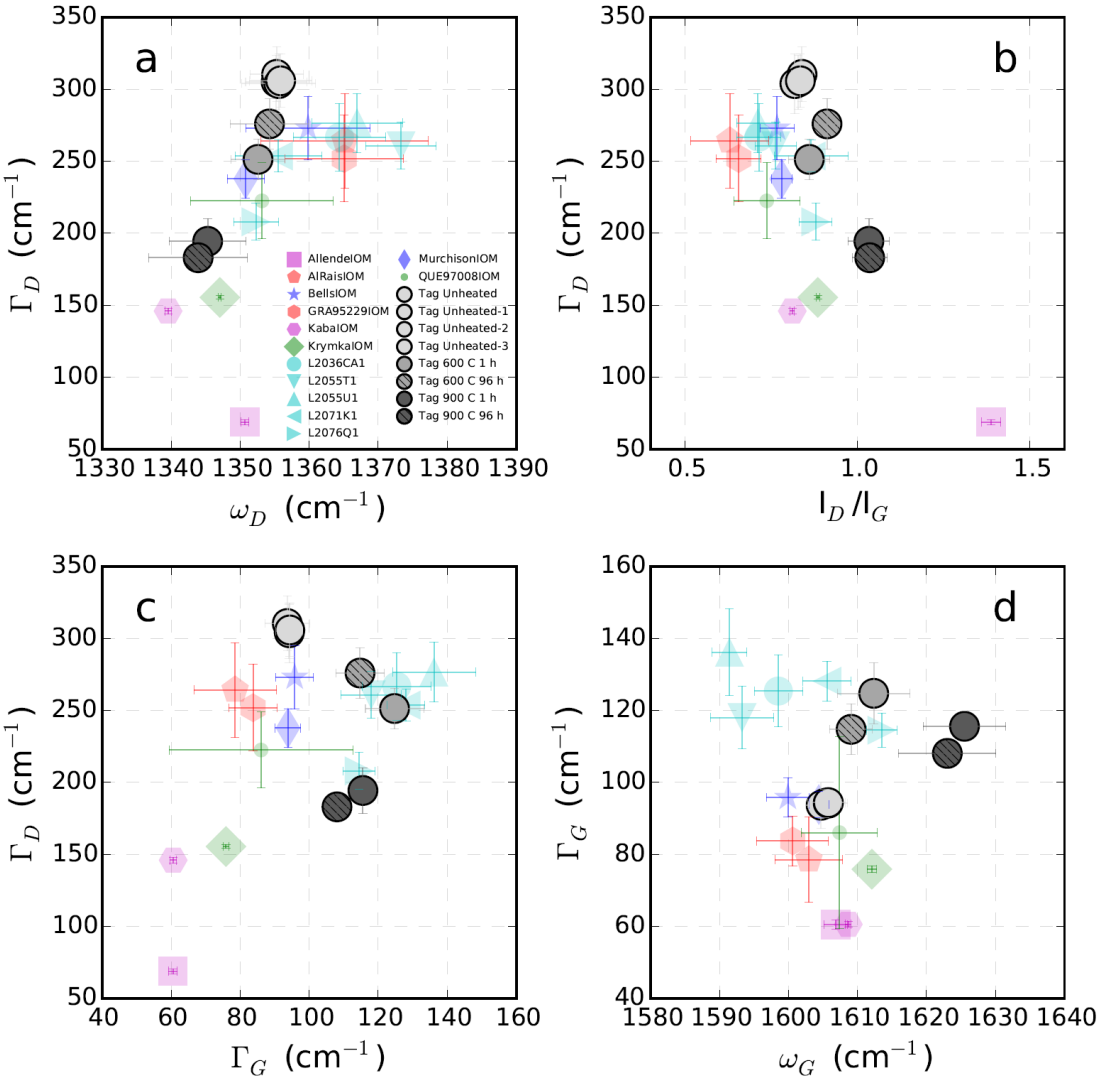

Figure 4. (a) Selected representative raw Raman spectra of the unheated and heated Tagish Lake meteorite samples. (b) The same Raman spectra which have been normalized with respect to the maximum intensity within the spectral range 1580–1630 cm^{-1}. The spectra have been offset vertically to enhance readability.

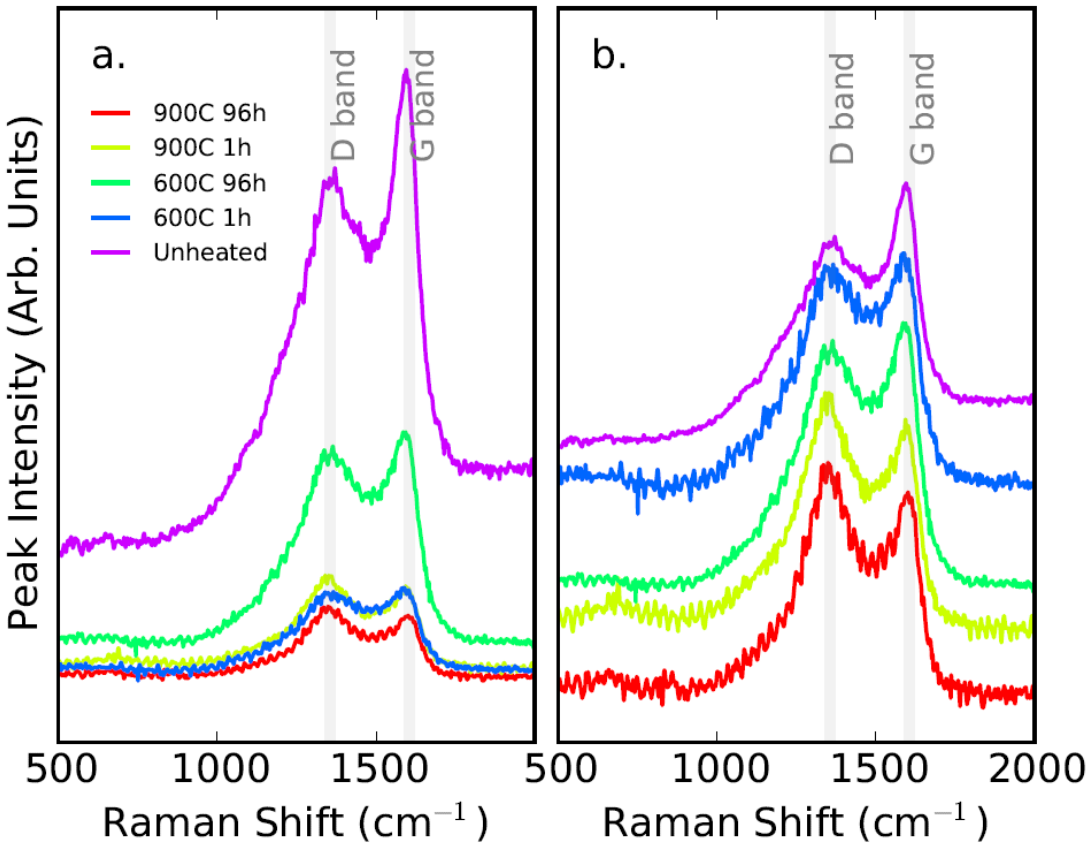

Figure 5. C-XANES spectra of different FIB sections from the Tagish Lake meteorite samples before and after heating to 600° and 900°C for 1 and 96h, obtained on separate dates. The spectra are presented in two subplots: (a) spectra are grouped according to the heating conditions, and (b) spectra are grouped according to different analytical dates. The spectra have been offset vertically to enhance readability.

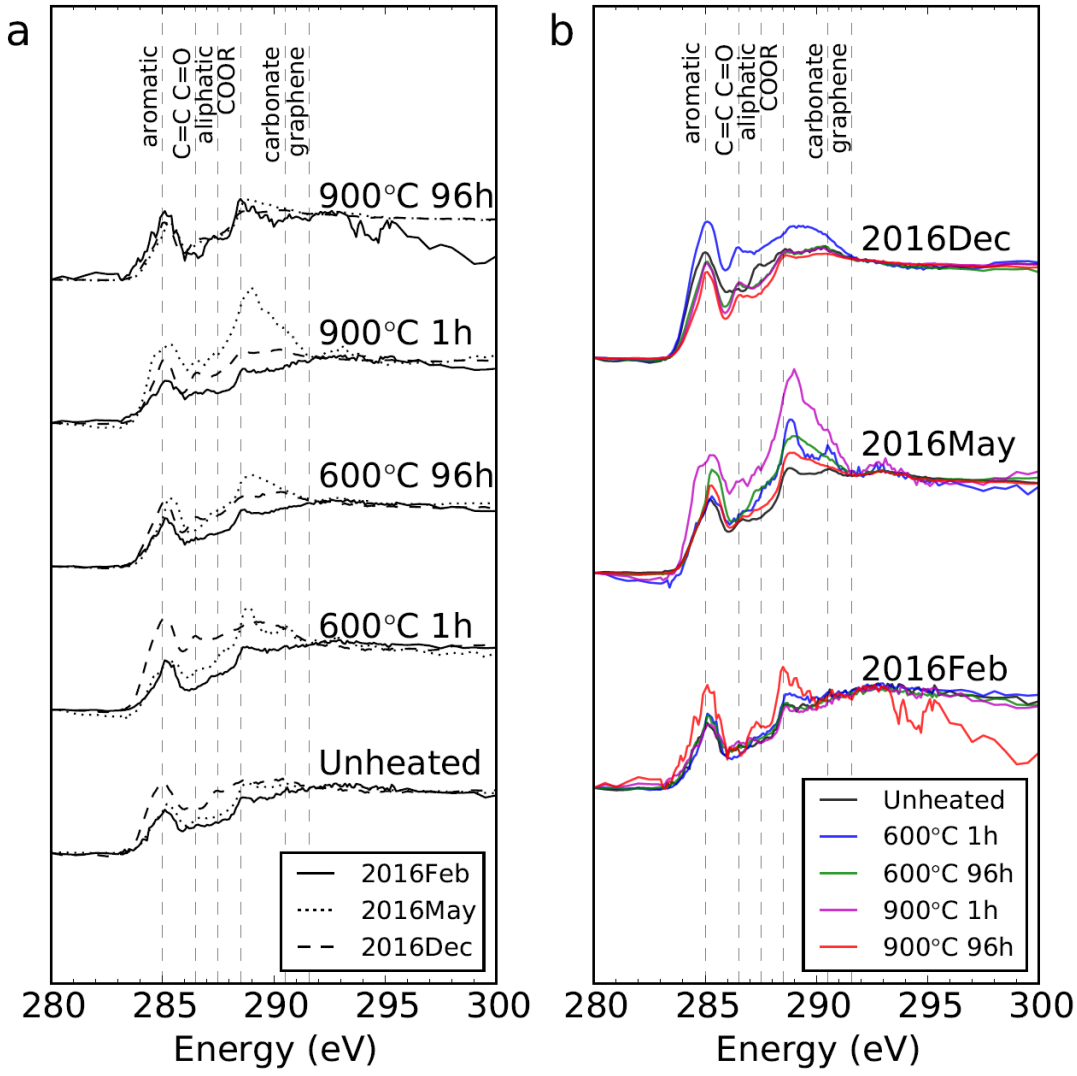

Figure 6. Comparison of the C-XANES peak area ratios between the IOM in Tagish Lake samples at different experimental heating conditions. Error bars are the standard deviation of the mean of the three FIB sections prepared for each experimental condition, which represent sample heterogeneity. The C-XANES raw spectra were first normalized to the total amount of C (absorption from 283-292 eV). The spectra were then fitted with an arctangent function to model the absorption edge (the center position, amplitude and width of the arctangent function are fixed to 291.5 eV, 1.0, and 0.4 eV, respectively) (Bernard et al. 2010) and Gaussian functions with a fixed energy position and a constant width (0.4 eV below 295 eV and 2 eV above).

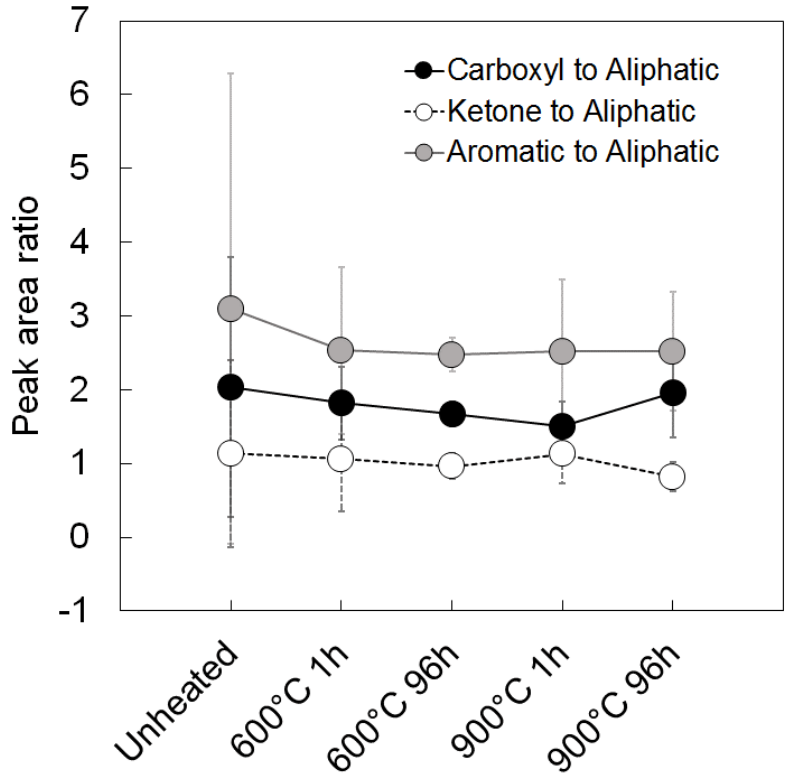

Figure 7. The relative amino acid abundances (relative to glycine) in the unheated and experimentally-heated Tagish Lake meteorite samples. Data of the aqueously altered lithology (#11i) of the Tagish Lake meteorite from Glavin et al. (2012) are shown here for comparison.

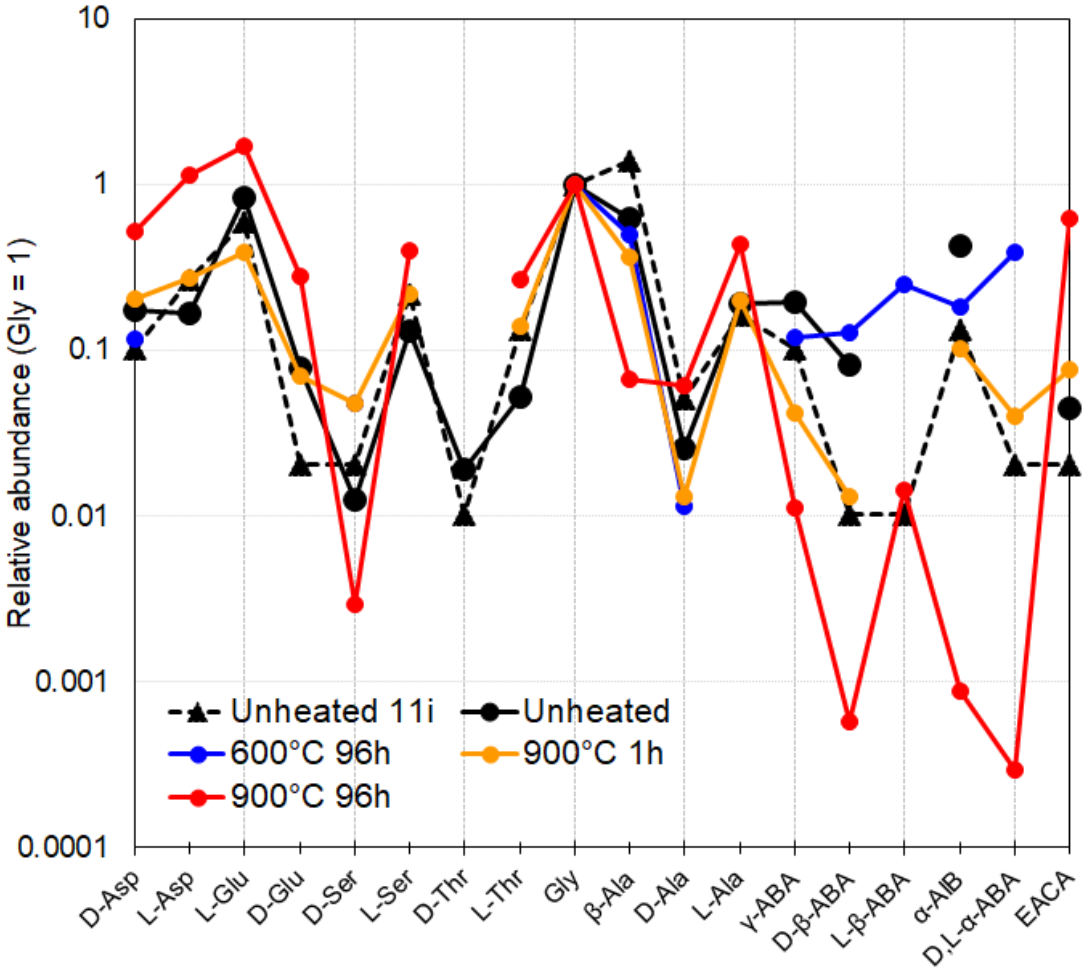

TABLE AND TABLE CAPTIONS

Table 1. Summary of the average abundances (in ppb) of identified amino acids in the blank-corrected 6 M HCl-hydrolyzed (total) hot-water extracts of the unheated and experimentally-heated Tagish Lake meteorite measured by UPLC-FD/QToF-MS.

	Unheated	600°C 96h	900°C 1h	900°C 96h	Unheated 11i[a]
D-Asp	3.8 ± 3.5	5.7 ± 2.9	6.3 ± 5.3	61.3 ± 49	<1
L-Asp	3.7 ± 0.3	n.d.	8.5 ± 0.6	132.9 ± 13.3	2.6 ± 0.5
L-Glu	18.3 ± 9.1	n.d.	12.2 ± 6.8	198.5 ± 108	<5.8
D-Glu	1.7 ± 0.8	n.d.	2.2 ± 2.3	32.2 ± 16.5	0.2 ± 1.6
D-Ser	0.3 ± 0.2	2.3 ± 2.4	1.5 ± 2	<0.7	<0.2
L-Ser	2.9 ± 0.5	n.d.	6.8 ± 1.6	46.9 ± 17.7	2.1 ± 0.9
D-Thr	<0.8	n.d.	n.d.	n.d.	<0.1
L-Thr	1.2 ± 0.1	n.d.	4.3 ± 3	30.9 ± 6.3	1.3 ± 0.4
Gly	21.9 ± 15.4	48.9 ± 47.3	31.1 ± 18.7	116.6 ± 114.1	9.7 ± 4.2
β-Ala	13.8 ± 1.3	24.4 ± 8	11.4 ± 4.1	7.8 ± 5.7	13.5 ± 0.7
D-Ala	<1.1	<1.1	<0.8	7.1 ± 0	<0.5
L-Ala	4.2 ± 0.3	n.d.	6.2 ± 0.2	50.3 ± 17.7	<1.6
γ-ABA	4.3 ± 2.1	5.8 ± 3.7	1.3 ± 0.5	1.3 ± 0.9	1 ± 0.5
D-β-ABA	<3.6	6.3 ± 8.1	0.4 ± 0.2	<0.1	<0.1
L-β-ABA	n.d.	<24.2	n.d.	1.7 ± 1.6	<0.1
α-AIB	9.3 ± 11.5	<17.6	3.1 ± 2	<0.2	1.3 ± 0.2
D,L-α-ABA	n.d.	<37.8	1.2 ± 1.7	<0.1	<0.2
EACA	<2	n.d.	2.4 ± 0.2	72.3 ± 41.5	<0.2
Total	**~89.1**	**~133.8**	**~99.4**	**~760.3**	**~41.5**
Total D-amino acids	**~8.5**	**~8.3**	**~33.8**	**~41**	**~12.1**

[a] The amino acids in the acid hydrolyzed hot-water extract of the aqueously altered lithology (#11i) of the Tagish Lake meteorite given by (Glavin et al. 2012) are shown here for comparison.

Abbreviations; Asp: aspartic acid, Glu: glutamic acid, Ser: serine, Thr: threonine, Gly: glycine, Ala: alanine, ABA: aminobutyric acid, AIB: aminoisobutyric acid, EACA: ε-amino-*n*-caproic acid.

SUPPLEMENTARY MATERIALS

for

Heating experiments of the Tagish Lake meteorite: investigation of the effects of short-term heating on chondritic organics

Queenie H. S. Chan[1]*†, Aiko Nakato[2], Yoko Kebukawa[3], Michael E. Zolensky[1], Tomoki Nakamura[4], Jessica A. Maisano[5], Matthew W. Colbert[5], James E. Martinez[6], A.L. David Kilcoyne[7], Hiroki Suga[8], Yoshio Takahashi[9], Yasuo Takeichi[10,11], Kazuhiko Mase[10,11] and Ian P. Wright[1]

*Corresponding author: Queenie H. S. Chan (E-mail: Queenie.Chan@open.ac.uk; Telephone: +1 (585) 653-6144).

This file includes:

Figures S1 to S5

Tables S1

Movies S1 to S2

Figure S1. EDX X-ray maps of the carbonate-poor lithology. Scale bar is 100 µm.

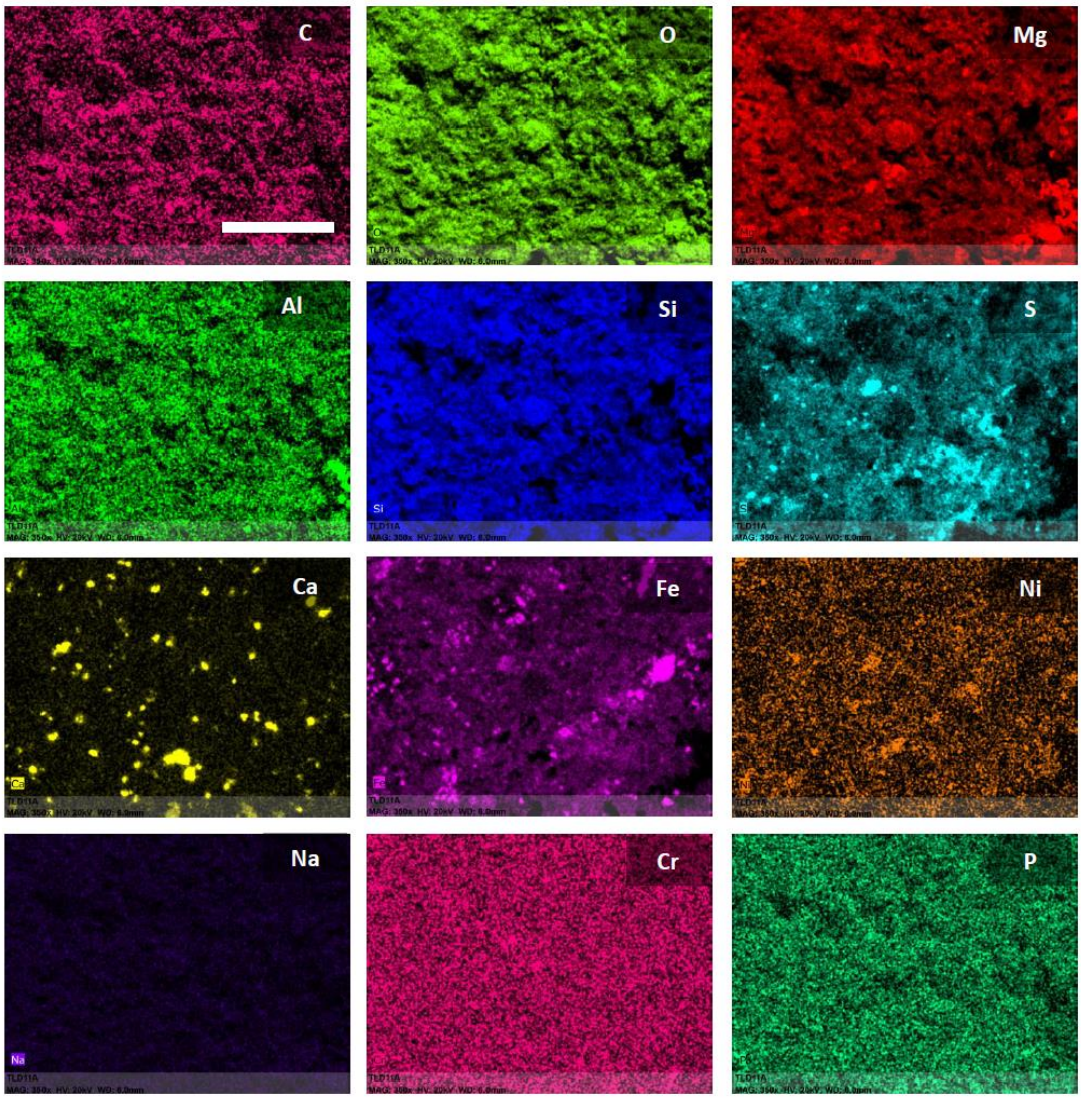

Figure S2. Peak-fitting results obtained with LBWF curve-fitting model in the first-order region (1000–1800 cm^{-1}) of the unheated Tagish Lake meteorite sample showing (top) the linear-background-corrected data (●), the fitted spectrum (black smooth solid line) and the decomposed D (green dashed line) and G (red dashed line) bands, (middle) the raw spectrum, and (bottom) the spectral fitting residue.

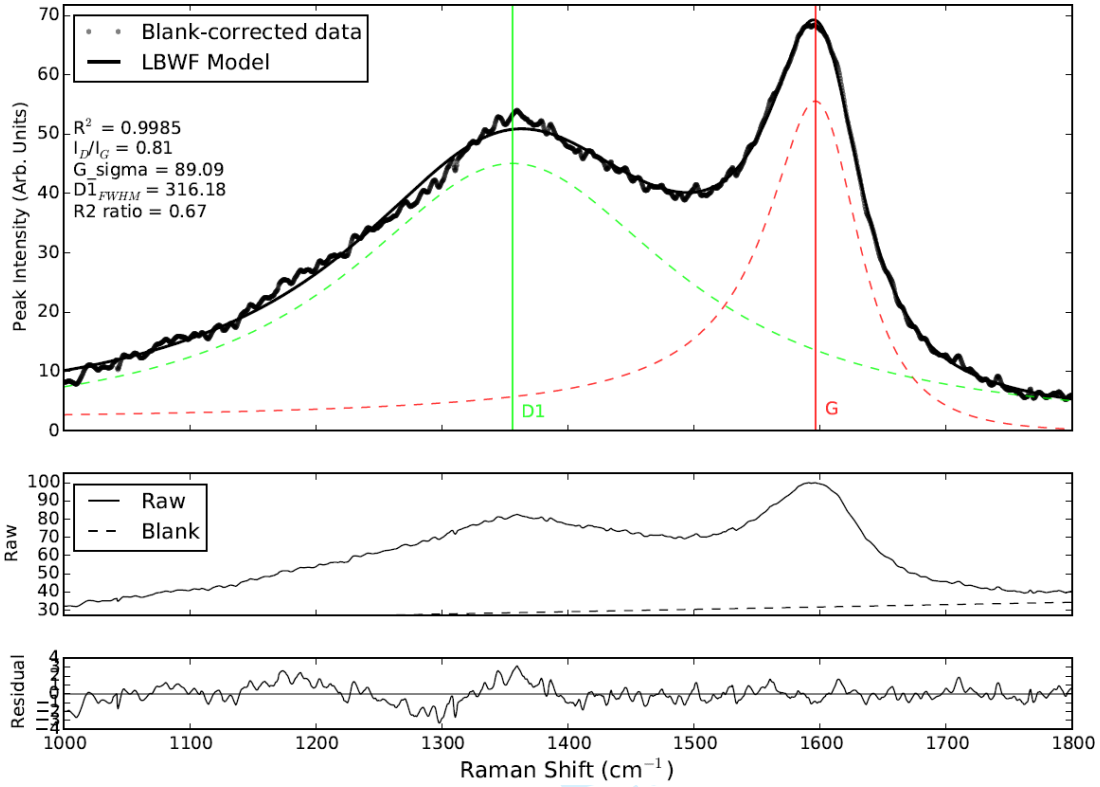

Figure S3. Comparison of the Raman band parameters of the unheated and experimentally-heated Tagish Lake samples obtained by LBWF and 2-Lorentzian (2L) peak-fitting models.

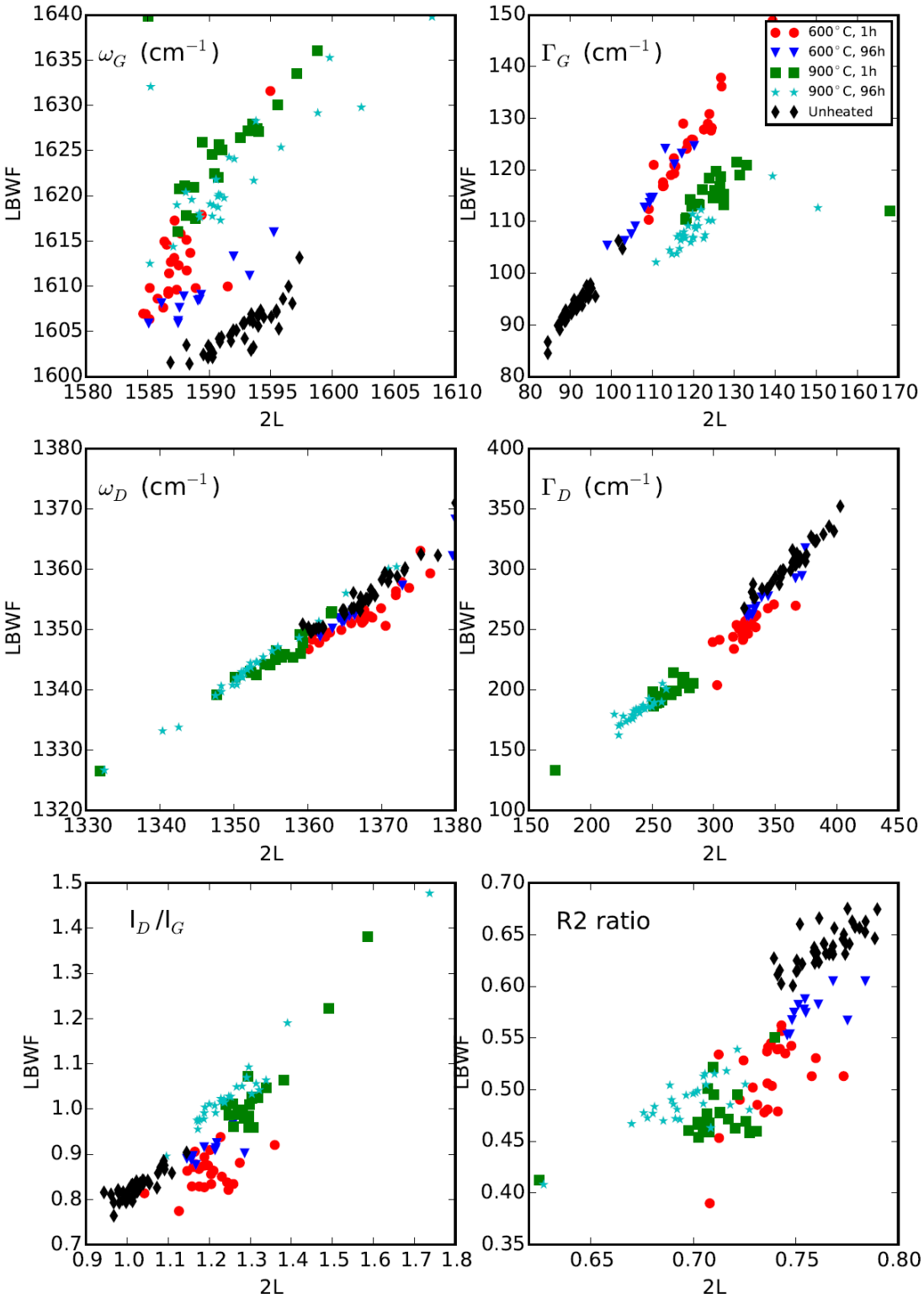

Figure S4. C-XANES spectrum and the spectral fitting procedure from the Tagish Lake meteorite sample (600°C 96h heating experiment) obtained from the FIB section prepared and analyzed on 2016 Feb. The top subplot shows the various Gaussian functions used to model the absorption of known functional groups and their set and actual fitted peak center locations. The middle subplot shows the arctangent function used to model the absorption edge. The bottom subplot shows the spectral fitting residue.

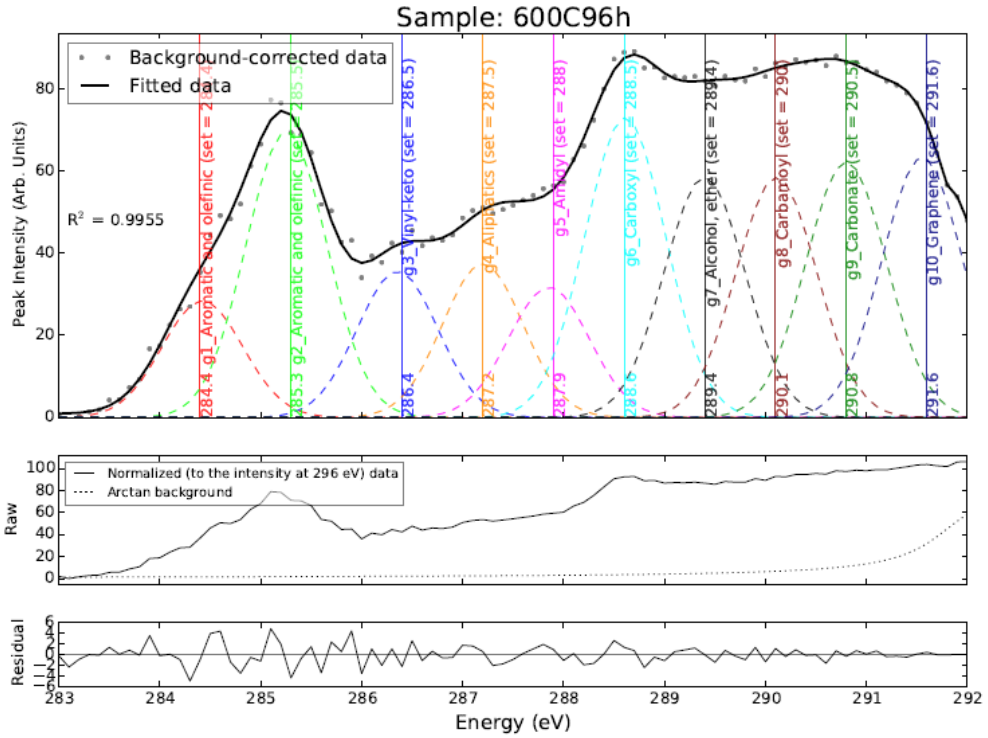

Figure S5. Comparison of the signal intensity between the raw Raman spectra of the unheated and heated Tagish Lake meteorite samples.

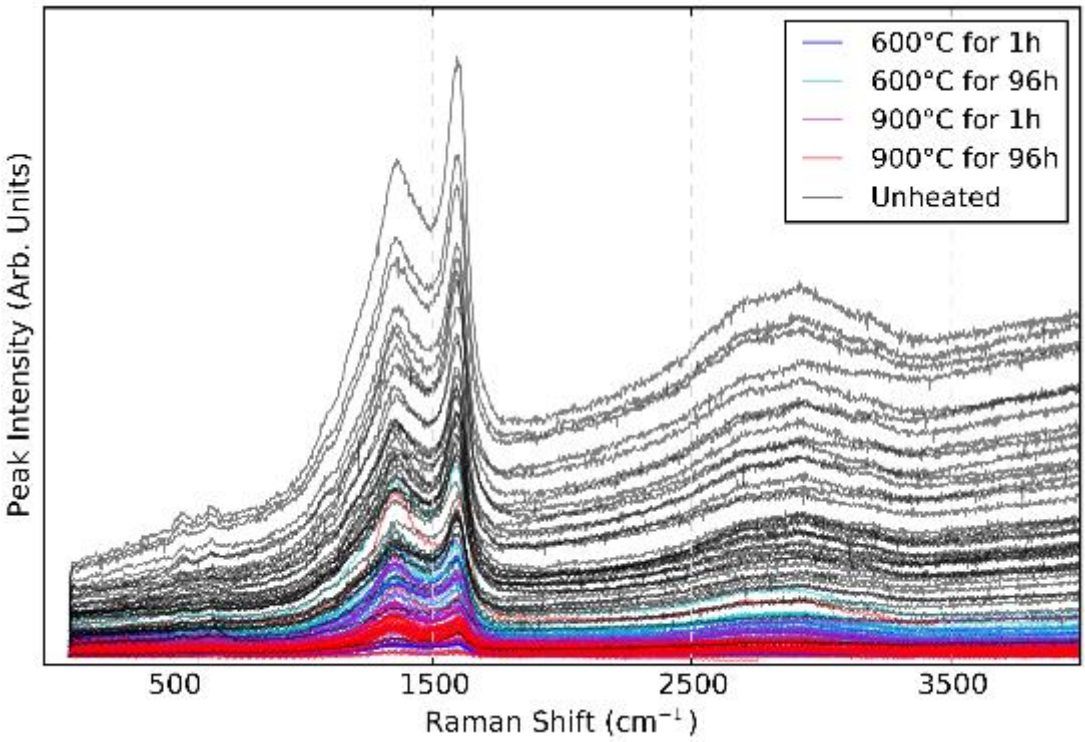

Table S1. Comparison between the Raman peak parameters of the Tagish Lake meteorite between different studies.[a]

	ω_G	ω_D	Γ_G	Γ_D	I_D/I_G	**Peak fitting model**
Quirico et al. 2014	1590.6 ± 3.0	1371.1 ± 4.1	102.9 ± 5.6	247.1 ± 10.3	0.80 ± 0.05	LBWF
Busemann et al. 2007	1580.6 ± 0.2	1350.5 ± 0.2	94.7 ± 0.1	311.4 ± 0.2	1.02 ± 0.05	2-Lorentzian
Matrajt et al. 2004	1593.9 ± 1.5	1378.8 ± 7.3	88.6 ± 7.5	328.1 ± 19.2	0.85 ± 0.06	2-Lorentzian
Nakamura et al. 2002	1591.8 ± 0.9	1381.5 ± 2.6	86.0 ± 3.3	283.9 ± 12.6	2.61	2-Lorentzian
This study	1605.3 ± 2.5	1355.2 ± 4.4	94.2 ± 4.0	304.9 ± 18.7	0.83 ± 0.02[b]	LBWF

[a]Uncertainties are 1σ standard deviation of the mean.

[b]The uncertainty for I_D/I_G represents the propagation of error.

Movie S1. Stack of the two-dimensional (2D) axial images of the Tagish Lake meteorite sample (#11).

Movie S2. 3D volumetric reconstruction of the Tagish Lake meteorite sample (#11).

Dear Drs. Jull and Sandford,

Thank you very much for handling the editorial process of our manuscript. We have considered all of the comments provided by the reviewer, and revised our manuscript accordingly. Below, please kindly find our point-by-point responses to the suggestions and comments on our manuscript.

Yours sincerely,

Queenie Chan

Our responses to Dr. Cody's comments:

1) Note that on Page 23 line 624 it is noted that Cody et al. 2008 flash heated to 600, 1000, and 1400 °C for 2 seconds in helium- this is correct, but they also did long term heating at 600, 800, 1000 and 1200 in argon up to 6 hours.

- We have modified the sentence into the following:
- "As noted by Cody et al. (2008b), Murchison IOM samples flash heated for up to two seconds at 600°, 1000°, and 1400°C in helium, and up to six hours at 600°, 800° and 1000°C in argon, all exhibit a systematic increase in the intensity of the 1s−σ* exciton at ~291.6 eV."

2) Figure 2: …review a little about what the mineralogy tells us about the environment during heating, e.g. reducing or oxidizing.

- We have modified Figure 2 to show the sample before and after the heating experiment of 900°C for 96h (instead of 600°C for 1h) to make it more consistent with the text.
- We have added the following sentences to the text:
- "Therefore, while phyllosilicates (e.g. saponite and serpentine), magnetite and Fe-Ni sulfides are common mineral phases observed in the matrix of the carbonate-poor lithology of the Tagish Lake meteorite (Zolensky et al. 2002 MAPS), the Tagish Lake samples heated to 900°C show mineral assemblages of predominantly anhydrous silicates, metal and troilite, implying a reducing heating environment."
- We have changed the figure legend accordingly:
- Optical photos of the Tagish Lake meteorite sample before and after the heating experiment at 900°C for 96h. The sample shows significant weight loss (~20%) upon heating which indicates the dehydration of phyllosilicates. Common mineral phases observed in the matrix of the unheated carbonate-poor lithology of the Tagish Lake

meteorite such as phyllosilicates, magnetite and Fe-Ni sulfides were converted into anhydrous silicates, Fe-Ni metal and troilite via dehydration and reduction.

3) Figures 3 & 4: "I don't think that anyone really knows exactly what controls D and G band widths, other than higher degrees of crystallinity should favor narrower Raman bands."
"The challenge with Raman has always been that there is no clear functional group level correlation with D and G band features."
"Raman trends are simply trends and are not rigorously tied to specific molecular structural characteristics"

- We have added the following sentences to the text:
- "The challenge with Raman analysis is that there is no clear functional group level correlation with Raman parameters, unlike XANES analysis which can directly attribute the absorption features to a certain chemical moieties. Therefore, the present data underscore the fact that the trend observed for different Raman parameters of chondritic IOM is not rigorously tied to one specific molecular structural characteristic.
- Despite the complicated influences of varying molecular structures to the Raman parameters, we can appreciate that a certain structural variation can lead to the development of several trends. One confident link is that higher degrees of crystallinity (ordering) favor the development of sharper bands."

4) Clearly there is something different between laboratory heating and natural heating and I suspect it might be confining pressure. I recommend that the authors discuss these unexpected trends in relation to what is observed in naturally thermally evolved IOM.

- We have added a paragraph to discuss immediately after the first mention of the variation between the G parameters of laboratory heated sample and meteoritic IOM (naturally heated sample):
- "Other than the disparity between the natures of the OM precursors, the difference between the trends observed for the G band parameters of the OM heated under laboratory and natural processes suggests variations in their heating conditions, such as the abovementioned heating kinetics and the confining pressure. IOM metamorphosed naturally at depth on a chondritic parent body up to kms in radius would have an overburden pressure significantly higher than the laboratory experimental condition (Asphaug et al. 2002). High pressure enhances the thermal transformation of organic C by reducing the temperature of graphite formation and accelerating the graphitization process, leading to the formation of graphite through gradual loss of hydrogen and other heteroatoms and annealing of structural defects (Davydov et al. 2004)."

5) Note that in Cody et al. 2008 only C-XANES were studied identifying the progressive generation of graphene like features and although C-XANES were compared with

Raman features (for natural samples) no Raman data were collected on the laboratory heated samples. It is quite likely that Raman data on pure IOM heated in the laboratory will show the same confusing G band behavior as seen in the present manuscript.

- We have added the following to the manuscript:
- "Although Cody et al. (2008b) observed a good correlation between the intensity of the 1s−σ* exciton and Raman spectra parameter, the C-XANES data of the experimentally heated IOM samples were compared with previously published Raman data (ΓD and ΓG) of chondritic IOM. Therefore it could be possible that by comparing both the C-XANES and Raman data of the same laboratory heated IOM would give the same trend we observed in this study."

6) Figure 5: I am confused as to why the spectra would change from Feb, May and Dec. The variation is not at all systematic, for example the 900 °C 96 hour looks more like the unheated than do any of the others. The only thing I might suggest is that the differences are more related to variations in beam line characteristics rather than the actual IOM chemistry. (note: we don't actually know how intense the C-XANES spectra are, nor what the base line absorption is- but the S/N suggests that carbon absorption is weak). When C-XANES features are very weak and X-ray beam drift is high (note the X-ray beam can move around), temporal variations in I0 scans can occur due to variation of carbon back ground on mirrors and monochromator. I would recommend that the authors compare their I0 scans for those dates to see if there are any differences (the C-XANES spectra are A= – log(I/Io) so variation of either "I" or "Io" can change "A".

- We have examined background effect to avoid the dependences of experimental devices and beam quality. All C-spectra were obtained with I0 at the same time, and subtract the "I0" from "I" after every experiment.
- We have also cross-checked the I0 data and confirm that the I0 data are not the culprit for such variation. Rather the sample heterogeneity is large, sometime even a single FIB section has heterogeneity depending on the ROI.
- We have discussed the unsystematic variation may reflect the original heterogeneity in the TL sample, since Feb, May, and Dec. samples were prepared from different area in the same heated/unheated sample chip.
- We have added the following to the manuscript:
- "The C-XANES spectra were corrected with background and analyzed by the subtraction of a linear regression using aXis2000 software, and then normalized to the intensity at 292 eV."

7) Three diagnostic XAS features: the development of a sharp peak at 291.6 eV and, the development of a pronounced broader peak at 292.3 eV and, the development of graphene-like EXAFS ocillations spanning out to 390 eV +.

- We have added the following to the manuscript:

- "In addition to the sharp peak around 291.6 eV, a pronounced broader peak at ~292.3 eV and graphene-like oscillations spanning out to 390 eV in extended X-Ray absorption fine structure (EXAFS) are also indicative of the development of graphene when studying with X-ray absorption spectroscopy (XAS) (G. Cody, personal communication, 2018)."

8) A sample of Tagish Lake from an altered clast (probably more similar to 11h- see Herd et al. 2012 and Alexander et al. 2014).
Why TL would behave so differently than Murchison IOM is not clear to me, but It is possible that the highly altered and aromatic rich Tagish Lake (the lithology studied here- more like TL 11v than 5b – see Herd et al) has lost the capacity to transform as Murchison IOM does towards more graphene like material because a lack of aliphatic carbon to begin with. If this is so, then it is suggests that different thermal pathways lead IOM to different outcomes.

- We have previously discussed that the TL sample we analyzed is more like the aqueously altered lithology, based on the amino acid content: "*The total amino acid abundance (free + bound) of the identified amino acids in the unheated Tagish Lake sample was about 89 parts-per-billion (ppb), which is consistent with the low amino acid abundance observed for the aqueously-altered lithology of the Tagish Lake sample (sample 11i, 40–100 ppb) and other TMCCs (e.g. Y-980115 ~300 ppb) in the literature*".
- We have also discussed the possible explanation for the disparities between the Murchison and Tagish Lake IOM in response to heating. We agree with the reviewer that the low capacity to transform due to the initially high aromatic content of the TL IOM is also a possible reason. In order to emphasize this, we have added the following sentences to the manuscript:
- "(Tagish Lake specimens showing an increasing degree of aqueous alteration: 5b [the least aqueously altered] < 11h < 11i < 11v [the most aqueously altered])"
- "The highly aromatic rich nature of the OM suggests that this Tagish Lake sample is more comparable to the aqueously altered specimens such as 11v and 11i rather than 5b analyzed in previous studies (e.g., Herd et al. 2011)"
- "We discuss here two possible explanations for the Tagish Lake IOM to behave so differently than Murchison IOM. First, the capacity for the highly altered and aromatic-rich IOM in the Tagish Lake sample (comparable to Tagish Lake specimens 11v and 11i) to further transform into graphene like material is limited as there is a lack of aliphatic C to begin with (Figure 5 and Figure 6). Second, ….."

9) Figure 6: It is true that C-XANES can be very subtle. For example if during heating one simultaneously loses aliphatic carbon (reducing intensity at ~ 287.3 eV) while increasing the size of polycyclic aromatic domains (increasing the number of π* states, then aromatic 1s- n*intensity will increase across the C-XANES spectrum. That is at energies spanning from 285 eV up to 289 eV. Thus, the apparent lack of trends in peak area ratio, may be hidden by molecular transformation into

polycyclic aromatic hydrocarbons. Note: benzene has 3 π* states, naphthalene has 5 π* states, anthracene has 7 π* states …etc.

- We agree with the referee on this and have added the following sentences to the main text of the manuscript:
- "Nevertheless, the apparent lack of trends in the peak area ratio may be hidden by molecular transformation into polycyclic aromatic hydrocarbons (PAHs) that shows several resonances at the range of 285–291 eV, in addition to main π* transition at ~285 eV. For example, the 285–291 eV regions of the C-XANES spectra of benzene (which has 3 π* states) and anthracene (which has 7 π* states) are distinct from each other, as benzene has several minor peaks between 287–291 eV in addition to a prominent broad peak at ~285 eV, whereas anthracene is comparatively featureless between 287–291 eV while the main feature at ~285 eV is shown as two smaller peaks at around 284 and 286 eV respectively (Gordon et al. 2003). Therefore, while the intensity at ~287.5 eV is reduced in response to the loss of aliphatic carbon in response to heating, heating also simultaneously increases the size of polycyclic aromatic domains (increasing the number of π* states) that show different resonances across the 285–291 eV region of the C-XANES spectrum, which could then lead to a non-systematic variation in the peak area ratio."

10) Figure 7 and Table 1:

These data must be considered with considerable suspicion as it is not at all expected that any amino acids would be detected after heating to 600 °C, let alone 900 °C, for any period of time, let alone 96 hours.

One possibility, is that amino acids actually form from CO, N2, H2, …etc. during cooling from 900 °C to ambient, however, these amino acids (aspartate and glutamic acid) have significant enantiomeric excesses so somehow the formation of such EEs would involve a symmetry breaking that is not at all understood nor predicable.

I can only stress that these results are completely unexpected and if prove to be true, constitute an outstanding result. I would recommend that the authors introduce these data with caution, at least noting that these results are not expected.

- We have added the following discussion to the manuscript:
- "Amino acids can be decomposed at temperatures as low as 100°C (Pietrucci et al. 2018), while proteic-amino acids are typically more thermodynamically unstable than non-proteic amino acids (e.g. β-alanine, γ-aminobutyric acid [γ-ABA]) (Kitadai 2016). Therefore, heating up to 600–900°C is expected to destroy amino acids through processes such as decarboxylation, deamination and chain homolysis which can result in the formation of a variety of simple volatile organic compounds such as amines, carboxylic acids and hydrocarbons (e.g., Bada et al. 1995; Pietrucci et al. 2018; Ratcliff et al. 1974)."
- "These results are completely unexpected as any amino acid present in the samples are susceptible to thermal decomposition at high temperatures. One possibility of

the increase in the amino acid abundance subsequent to heating, is that amino acids are formed from simple precursor molecules such as CO, N2 and H2 which serve as feedstock for mineral-catalyzed Fischer Tropsch-type (FTT) reactions (e.g., Anders et al. 1973; Pizzarello 2012; Yoshino et al. 1971). The FTT reactions lead to the formation of primarily straight-chain amino acids (e.g. glycine, β-alanine, γ-ABA, ε-amino-n-caproic acid [EACA]) of which the amino group is on the carbon farthest from the carboxylic acid. However, when heated to 900°C, the minerals commonly associated with FTT reactions such as montmorillonite clay and magnetite are at expense to form anhydrous silicates, metal and troilite in the Tagish Lake samples (Figure 2). Although metals can also act as FTT reactions catalysts (Dry 2002), hydrogenation of CO to hydrocarbons is a very slow process in the absence of a suitable catalyst (Hayatsu and Anders 1981; Lancet and Anders 1970). The mineral phases of which the formation thresholds are above ~350–400K, such as olivine, Fe and FeS, are not effective catalysts for the FTT reactions, whereas the phases formed at lower temperatures (e.g. montmorillonite clay and magnetite) are. This elucidates a higher abundance of organic compounds in meteorites containing these mineral phases. Therefore, the formation of amino acids via the FTT reactions in the absence of these effective catalysts should be hindered rather than enhanced. When focusing on the yield of the four-carbon amino acids ABA, the abundances of the straight-chain γ-ABA are not always higher than that of the branched isomers in the heated samples (Figure 7), which again testify against the production of amino acids via the FTT reactions."